BAŞKENT UNIVERSITY INSTITUTE OF SCIENCE AND ENGINEERING DEPARTMENT OF ELECTRICAL-ELECTRONICS ENGİNEERING MASTER OF SCIENCE IN ELECTRICAL-ELECTRONICS ENGINEERING

NOTCHED PLANAR SQUARE MONOPOLE ANTENNA DESIGN BY USING ARTIFICIAL NEURAL NETWORK

BY

ERTUĞRUL ATILKAN

MASTER OF SCIENCE

ANKARA - 2022

BAŞKENT UNIVERSITY INSTITUTE OF SCIENCE AND ENGINEERING DEPARTMENT OF ELECTRICAL-ELECTRONICS ENGINEERING MASTER OF SCIENCE IN ELECTRICAL-ELECTRONICS ENGİNEERING

NOTCHED PLANAR SQUARE MONOPOLE ANTENNA DESIGN BY USING ARTIFICIAL NEURAL NETWORK

BY

ERTUĞRUL ATILKAN

MASTER OF SCIENCE

ADVISOR

DR. ÖĞR. ÜYESİ ALPARSLAN ÇAĞRI YAPICI

CO-ADVISOR

DR. ÖĞR. ÜYESİ MURAT ÜÇÜNCÜ

ANKARA - 2022

BAŞKENT UNIVERSITY
INSTITUTE OF SCIENCE AND ENGINEERING

This study, which was prepared by ERTUĞRUL ATILKAN for the program of Master's of Electrical and Electronics Engineering with Thesis, has been approved in partial fulfillment of the requirements for the degree of MASTER OF SCIENCE in Electrical and Electronics Engineering Department by the following committee.

Date of Thesis Defense: 13 / 09 / 2022

Thesis Title: Notched Planar Square Monopole Antenna Design by Using Artificial Neural Network

Examining Committee Members	**Signature**
Dr. Öğr. Üyesi Alparslan Çağrı YAPICI (Başkent Üniversitesi)	……..
Prof. Dr. Öğr. Üyesi Hamit ERDEM (Başkent Üniversitesi)	……..
Dr. Öğr. Üyesi Aykut YILDIZ (TED Üniversitesi)	……..

APPROVAL

Prof. Dr. Faruk ELALDI
Director, Institute of Science and Engineering

Date: ... /… / ……

BAŞKENT ÜNİVERSİTESİ
FEN BİLİMLERİ ENSTİTÜSÜ
YÜKSEK LİSANS TEZ ÇALIŞMASI ORJİNALLİK RAPORU

Tarih: 04/10/2022

Öğrencinin Adı, Soyadı	:	ERTUĞRUL ATILKAN
Öğrencinin Numarası	:	21910487
Anabilim Dalı	:	Elektrik-Elektronik Mühendisliği Anabilim Dalı
Programı	:	Elektrik-Elektronik Mühendisliği Tezli Yüksek Lisans Programı
Danışmanın Adı, Soyadı	:	Dr. Öğr. Üyesi Alparslan Çağrı YAPICI
Tez Başlığı	:	Notched Planar Square Monopole Antenna Design by Using Artificial Neural Network

Yukarıda başlığı belirtilen Yüksek Lisans tez çalışmamın; Giriş, Ana Bölümler ve Sonuç Bölümünden oluşan toplam 53 sayfalık kısmına ilişkin, 04/10/2022 tarihinde tez danışmanım tarafından Turnitin adlı intihal tespit programından aşağıda belirtilen filtrelemeler uygulanarak alınmış olan orijinallik raporuna göre, tezimin benzerlik oranı %15'dir.

Uygulanan filtrelemeler:

1.Kaynakça hariç

2.Alıntılar hariç

3.Beş (5) kelimeden daha az örtüşme içeren metin kısımları hariç

"Başkent Üniversitesi Enstitüleri Tez Çalışması Orijinallik raporu Alınması ve Kullanılması Usul ve Esaslarını" inceledim ve bu uygulama esaslarında belirtilen azami benzerlik oranlarına tez çalışmamın herhangi bir intihal içermediğini; aksinin tespit edileceği muhtemel durumda doğabilecek her türlü hukuki sorumluluğu kabul ettiğimi ve yukarıda vermiş olduğum bilgilerin doğru olduğunu beyan ederim.

Öğrenci İmzası:

ONAY

04/10/2022

Öğrenci Danışmanı

Dr. Öğr. Üyesi Alparslan Çağrı YAPICI

ACKNOWLEDGMENTS

I would like to thank my esteemed teacher and thesis advisor Assoc. Dr. Alparslan Çağrı YAPICI, my father Ömer ATILKAN, my mother Fadime ATILKAN and my brother Gökçen ATILKAN, who have always supported me throughout my education life, my dear colleagues Türker DİRLİK, Mustafa ÇERÇİ, who have always been with me and supported me throughout my graduate education and thesis studies, I would like to express my endless thanks to Mübarek Kaya and Serdar KAYA. I would also like to thank Osman ASLAN for his friendship and motivation during the writing of the thesis.

To my love İnci

ÖZET

ERTUĞRUL ATILKAN
Yapay Sinir Ağı Kullanılarak Çentikli Düzlemsel Kare Monopol Anten Tasarımı
Başkent Üniversitesi Fen Bilimleri Enstitüsü
Elektrik-Elektronik Mühendisliği Anabilim Dalı
2022

Bu çalışmada, çok katmanlı algılayıcı (MLP) modeline dayalı yapay sinir ağı, metal plaka çentikleri oyulmuş kare monopol antenin tasarımı için uygulanmıştır. Sinir ağını eğitmek için kullanılan Lavenberg-Marquardt (LM), ölçekli eşlenik gradyan (SCG), bayesian düzenlileştirme (BR) olan geri yayılım algoritmaları kullanılmıştır. Algoritmaların çıktıları elektromanyetik (EM) analiz programına aktarılarak simülasyon sonuçları karşılaştırılmıştır. Doğruluk, EM simülasyonları ve sinir ağı çıktısı arasındaki korelasyon ile hesaplanmıştır. Sinir ağını eğitmek için veri seti, bilgisayar destekli tasarım (CAD) yazılımları vasıtasıyla gerçekleştirilen anten benzetimleri ile oluşturulmuştur. Veri seti, L-bandı ve S-bandının frekans spektrumunun kritik tasarım parametrelerini yakalamak için oluşturulmuştur. Buna rağmen oluşturulan yapay sinir ağı bu bantların dışında da, doğruluğu EM simülasyon sonucu ile uyumlu anten tasarımları gerçekleştirebilmektedir. Sunulan sonuçlar, sinir ağının arzu edilen S-parametrelerine uygun anten tasarım gerçekleştirebildiğini göstermiştir. Ayrıca yapay sinir ağı antenin fiziksel tasarım parametrelerini antenin S-parametreleri üzerindeki etkilerini de kestirmektedir.

ANAHTAR KELİMELER: Lavenberg-Marquardt (LM), ölçekli eşlenik gradyan (SCG), bayesian düzenlileştirme (BR), ANN, çok katmanlı algılayıcı (MLP), Çentikli Düzlemsel Kare Monopol Anten

ABSTRACT

ERTUĞRUL ATILKAN

Notched Planar Square Monopole Antenna Design by Using Artificial Neural Network

Başkent University Institute of Science

Department of Electrical and Electronics Engineering

2022

In this paper, artificial neural network based on multilayer perceptron (MLP) model is applied to the metal-plate notches are carved into the square monopole antenna. Backpropagation algorithms that are Levenberg-Marquardt (LM), scaled conjugate gradient (SCG), Bayesian regularization (BR) used to train the neural network. The outputs of the algorithms were transferred to the electro-magnetic (EM) analysis program and the simulation results are compared. The accuracy is calculated by correlation between EM simulations and neural network output. In order to train the neural network, dataset is created by parametric analysis of the antenna design parameters in computer-aided design (CAD). Although the dataset is generated to capture critical design parameters of frequency spectrum of L-band and S-band, the out of band performance has a good agreement with the EM simulation result. The results presented indicate that the neural network can predict antenna design parameters by using S-parameters and effects of the design parameters of the antenna on the S-parameters.

KEYWORDS: Levenberg-Marquardt (LM), scaled conjugate gradient (SCG), Bayesian regularization (BR), ANN, multilayer perceptron (MLP), Notched Planar Square Monopole Antenna

INDEX

LIST OF TABLES

Page

LIST OF FIGURES

Page

LIST OF ICONS AND ABBREVIATIONS

FDTD	Finite-Difference Time-Domain
FE	Finite Element
ANN	Artificial Neural Network
MoM	Method of Moments
FECM	Foster Equivalent Circuit Model
BW	Bandwidth
DCS	Digital Cellular System
PCS	Personal Communications Services
DECT	Digital Enhanced Cordless Telecommunications
PHS	Personal Handy-phone System
IMT-2000	International Mobile Telecommunications-2000
WLAN	Wireless Local Area Network
CAD	Computer-Aided Design
LM	Levenberg-Marquardt
SCG	Scaled Conjugate Gradient
BR	Bayesian Regularization
f_l	Lowest resonant frequency
f_h	Highest resonant frequency
f_c	Merkez frekansı
RBFN	Radial Basis Function Network

1. Introduction

In order to reducing design process, synthesis and modeling of the antenna have become more important. There are many methods to analyze and synthesize the antenna such as finite-difference time-domain (FDTD) [1,2], finite elements (FE) [3], method of moments (MoM), genetic algorithms [4,5], and artificial neural network (ANN) [6-9]. The narrowband antennas' resonant frequency can be found accurately by computing antenna design formulas [6]. However, wideband antennas have a difficulty in determining resonant frequency. Several attempts tried to model broadband antennas such as Foster Equivalent Circuit Model (FECM) [10,11] and ANN [12-13]. In literature, ANN is applied to predicting the slot size on the radiating patch [12], circular microstrip antenna [7], equilateral triangular microstrip antenna [6].

Planar metal-plate monopole antennas are used to compete with these demands because those antennas are good at distributing omnidirectional pattern and broadband impedance matching [14-15]. Since having a basic shape, square monopole antennas have fewer antenna design variables compared to other types of planar monopole antennas. Square monopole antennas draw attention to enhance its bandwidth and radiation pattern. The square planar monopole antenna's impedance bandwidth has been improved through a number of experiments, including the use of a double feed [16], a semi-circular base [17], a beveling technique [18], a shorting pin [19], notches carved into the radiator [20]. The S band and L band have a frequency spectrum around 1.1 GHz to 4 GHz. This frequency spectrum is useful for telemetry applications, direction finding (DF), distance measuring system. Global positioning system is also important application. Mobile communication applications a such as DCS (1710–1880 MHz), PCS (1850–1990 MHz), DECT (1880–1900 MHz), PHS (1895–1920 MHz), IMT-2000 (1885– 2025MHz), UMTS (1920–2170 MHz), and WLAN (2400–2485 MHz) [21] are growing. In this work ANN is applied to notched planar metal-plate monopole antenna due to the antenna having so far been frequency tuned by optimizing. The number of parameters used to calculate the antenna's resonant frequencies grows as the number of notches carved into the radiating element increases because optimizing the antenna in computer-aided design (CAD) takes too much time. It was deemed necessary to create a mathematical and equivalent model for the proposed antenna. The suggested antenna model makes frequency adjustment via slots on the radiating metal-plate monopole. The analysis challenge in microstrip patch antenna that is modeled

by ANN can be described as determining the resonance frequency for a given dielectric material and geometric structure [13] whereas in this work, the corresponding ANN model focuses on determining antenna dimensions as a function of resonant frequency and bandwidth. In this thesis, ANN training algorithms, Levenberg-Marquardt (LM), scaled conjugate gradient (SCG), and Bayesian regularization (BR) algorithms are employed to the proposed antennas in L-band and S-band. The algorithm's accuracy performance is compared at in-band and out-of-band. The results have a good agreement between EM simulations and predicted ANN output.

2. Planar Square Monopole Antenna

G. Dubost and S. Zisler initially described the planar monopole antenna in 1976 [2]. It is achieved by substituting a traditional wire monopole with a planar monopole, which is positioned above a ground plane and typically supplied with a coaxial probe [1]. The square planar monopole antenna has the simplest geometry of all the planar monopole antennas, and its radiation pattern is less damaged within the impedance bandwidth. Because the planar monopole only has a 2:1 impedance bandwidth ratio, these favorable characteristics draw many investigations, mostly on bandwidth improvement. The impedance matching can be affected by the antenna geometry, the feed gap, the position of feed, and the geometric form of the monopole's feed side. Square planar monopole antennas are straightforward to make from a single metal plate and have a basic shape. However, among the different forms of planar monopole antennas, the square planar monopole antenna has the disadvantage of having a lower impedance bandwidth [3, 4]. Square monopole antenna is shown below as Figure 2.1.

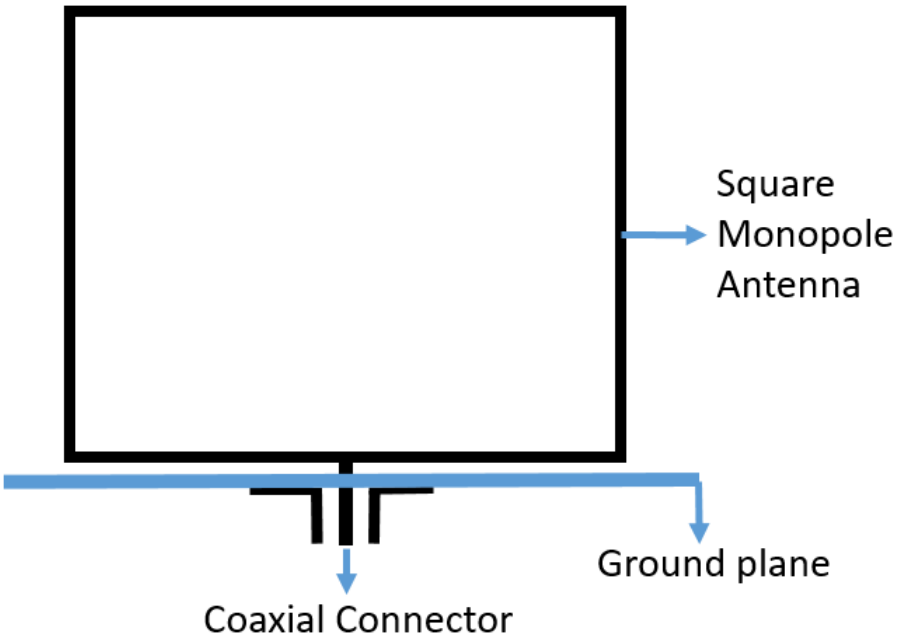

Figure 2. 1 Square Monopole Antenna

The impedance bandwidth of the square planar monopole antenna has been improved using a number of bandwidth augmentation techniques, including the use of a double feed [2], a semi-circular base [5], a beveling technique [6], a shorting pin [7], trapezoidal monopole antenna[23], square monopole antenna[24], circular disc monopole antenna[24], Planar inverted cone antenna[25], leaf shaped planar inverted cone antenna[26]. Figure

2.2,3,4,5,6 show some of these antenna geometries and their bandwidth. The bandwidth ratios of these monopole antennas can reach 22.8:1. Figure 2.1 shows vertical trapezoidal monopole antenna. The antenna consists of a trapezoidal radiator above a ground plane. The pattern will be significantly impacted by the size of the ground plane, particularly in the azimuthal plane. The antenna can be excited with a coaxial cable through a surface-mount SMA (Subminiature version A) connector.

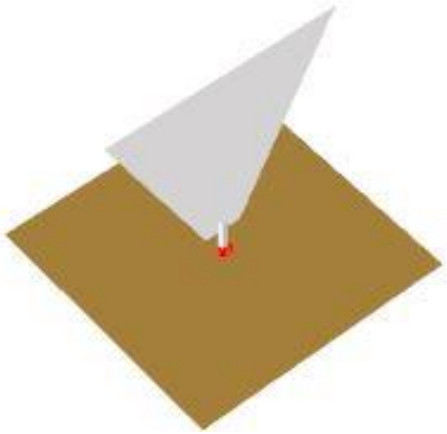

Figure 2. 2 Vertical trapezoidal monopole antenna

Figure 2.3 shows square monopole antenna with trident-shaped feed. The antenna consists of a rectangular monopole antenna with trident-shaped feed radiator above a ground plane. The size of the rectangular monopole is determined by the lowest operating frequency.

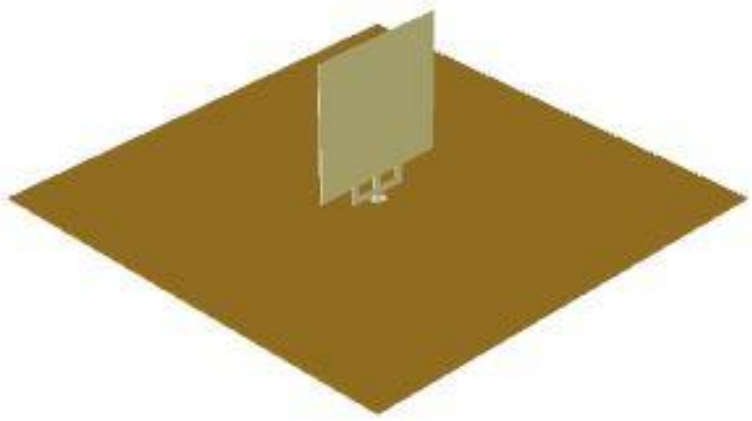

Figure 2. 3 Square monopole antenna with trident-shaped feed

Figure 2.4 shows circular disc monopole antenna. The antenna comprises of a ground plane and a circular disc radiator. A fundamental monopole's wire is switched out for a circular conducting disk, creating a circular disk monopole with an exceptional impedance bandwidth of 1:8 [14].

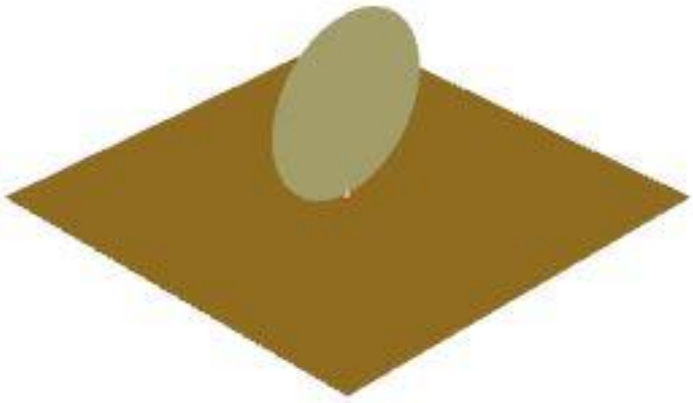

Figure 2. 4 Circular disc monopole antenna

Figure 2.5 shows planar inverted cone antenna. The antenna consists of inverted cone radiator above a ground plane. The size of the planar inverted cone antenna is determined by the lowest operating frequency.

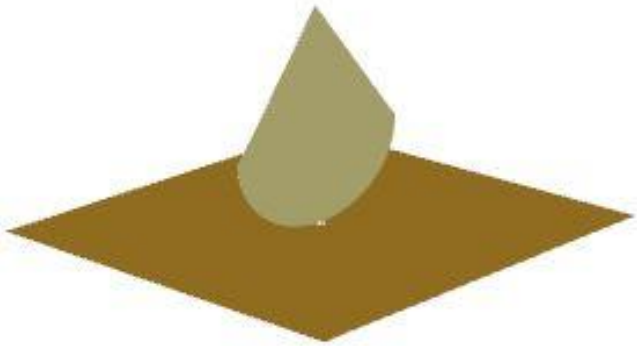

Figure 2. 5 Planar inverted cone antenna

An inverted cone antenna with a leaf shape is depicted in Figure 2.6. A ground plane is above an inverted cone radiator that serves as the antenna. The radiator of a leaf-shaped planar inverted cone antenna includes holes, which is the only distinction between it and a regular planar inverted cone antenna.

Figure 2. 6 Leaf shaped planar inverted cone antenna

Four more holes enable a very wide ohmic resistance information measure of bandwidth while reducing the overall size of the antenna. These antennas are placed on top of a ground plane and are primarily flat with an oval shape and an inverted top construction. The structure has four holes that are part of the diverging construction. These antenna types can be designed along a certain frequency band. Due to this situation, the bandwidth remains narrow. In addition, it does not perform well in impedance matching. This causes low antenna gain. Notched metal-plate square monopole antenna gets ahead of other antennas due to its easy fabrication and easy impedance matching. Comparing this type of antenna to other planar monopole antennas, it is preferable for constructing a monopole antenna with a wider band and higher gain. Moreover, notched metal-plate square monopole antenna is low profile and low volume compared to other types of monopole antenna.

2.1. Design of Notched Metal-Plate Square Monopole Antenna

Figure 3.1 shows the proposed Notched Planar Square Monopole's geometry. The radiating element, ground plane, and SMA connector are the three components that make up the antenna model. A planar square monopole serves as the radiating component. In this example, the planar square monopole is connected to a SMA connector and is located above a ground plane [22]. The planar square monopole antenna is manufactured from brass thickness of 0.5mm to solder it to SMA connector easily. The ground plane is manufactured from aluminum which has a square shape dimension of *S*. The radiating element has three design parameters: length of the antenna (LM), length of the notch (NL) and width of the notch (NW). Due to the geometry of square, width of the radiating element is also equal to length of the antenna. Notches are carved into radiating element in order to decrease Q value resulting with increasing antenna bandwidth [20]. Figure 2.7 shows the general Notched Planar Square Monopole Antenna design:

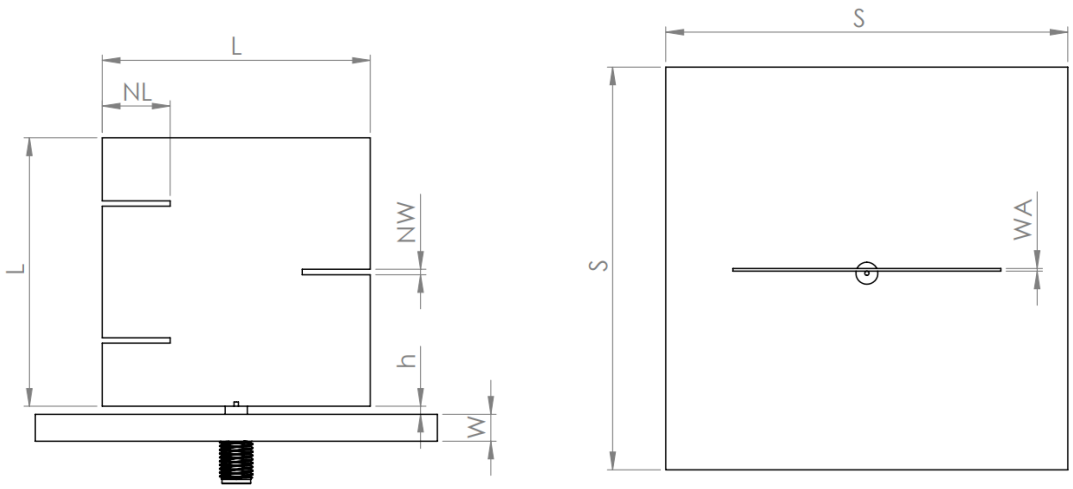

Figure 2. 7 The drawing of the proposed antenna model

Where WA is the antenna's thickness, W and S are the ground plane's thickness and length, respectively, and h is the distance between the antenna and ground plane. Cylindrical wire antennas can be used to determine the frequency of square monopole antennas that corresponds to the first lower edge of the bandwidth. Here cylindrical antenna should have the the height L with equivalent radius, resulting the same are with square monopole antenna [27]. For real input impedance, the length of the monopole can be calculated as [34],

$$L = 0.24 * \lambda * \mathrm{F} \tag{2.1}$$

Where F can be calculated as,

$$F = (L/r)/(1 + \frac{L}{r}) \tag{2.2}$$

The resonant frequency (fr) can be determined as,

$$fr = \left(\frac{c}{\lambda}\right) = (30 * 0.24)/(\mathrm{l} + \mathrm{r})\ \ \mathrm{GHz} \tag{2.3}$$

As can be seen from Figure 3.1, there are three important antenna design parameters. In order to use to ANN to predict antenna operating frequency, parametric analyzes were carried out. To make it clear, parametric analyzes can be called as monitoring the antenna performance on changing the antenna design parameters' values. For example, when the antenna length is 50 mm, it is decided by looking at the S_{11} value, at which intervals the antenna will be simulated. In other words, some trials are done to monetarize antenna design parameter' values are suitable to use them. Simulations are conducted for different values of notch length and notch width in order to training dataset. It is done for the notch length and

notch width antenna design parameters. Briefly, these antenna design parameters first applied to HFSS antenna design which is showed in Figure 2.7. Then, the output of the HFSS simulation results manufactured training dataset. operation also done for the create ANN training stage that will be explained next chapters.

2.2. Increasing Number of Notches

The effect of increasing the number of notches, which is one of the antenna design parameters, on the antenna results was investigated. The investigation is done for antenna without notch, 1-notch, 2-notch, 3-notch and 4-notch. 1- notch is created from antenna without notch by adding a notch on the radiator. This operation is also done for the 2-notch, 3-notch and 4-notch antennas. The length, notch length and notch width are stayed the same. Moreover, distance between the notches is also the same in all designs. The investigation is done with monitoring surface current distribution and S_{11}. Surface current distribution in antennas is one of the important parameters in the design of the antenna. In previous studies, notches were used to reduce the antenna size. It is considered that the current through the notch increases the current density due to the capacitive effect. Since the electrical length decreases, the current density increases. Thus, the Q value decreased, and the bandwidth increased [20]. In Figure 2.8, the antenna without the notch and the antenna with the three notches are evaluated in the S_{11} (dB) graph. Notched antenna surface current results are given for antenna without the notch, one notch, two notches and three notches.

Antenna designs have been taken care to operate in the same frequency bands, no change has been made in antenna length, only the number of notches has been increased. Simulation results are given form of surface current distribution and S_{11} result of the antenna obtained without notch. The surface current distribution for the antenna without notches is shown in Figure 2.8.

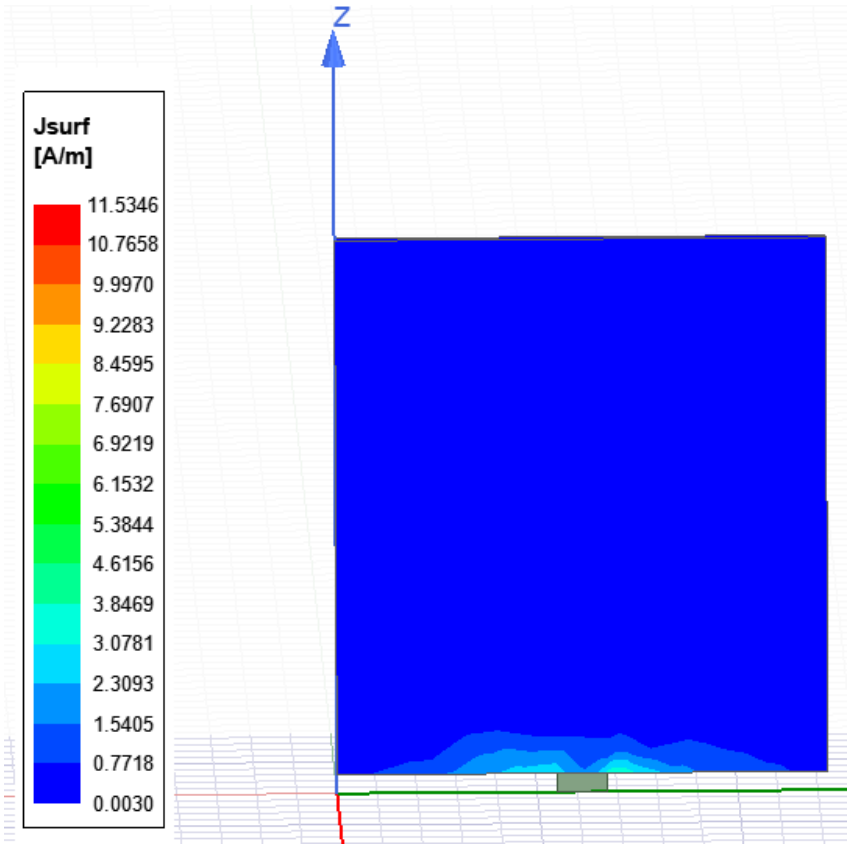

Figure 2. 8 Surface current distribution if the notches are not carved

One can claim from the Figure 2.8, surface current distribution is extremely low. Since there are no notches, the current distributions on the antenna are usually close to the sharp ends observed in the regions. Figure 2.9 is used to show the return loss graph of square monopole antenna without notch.

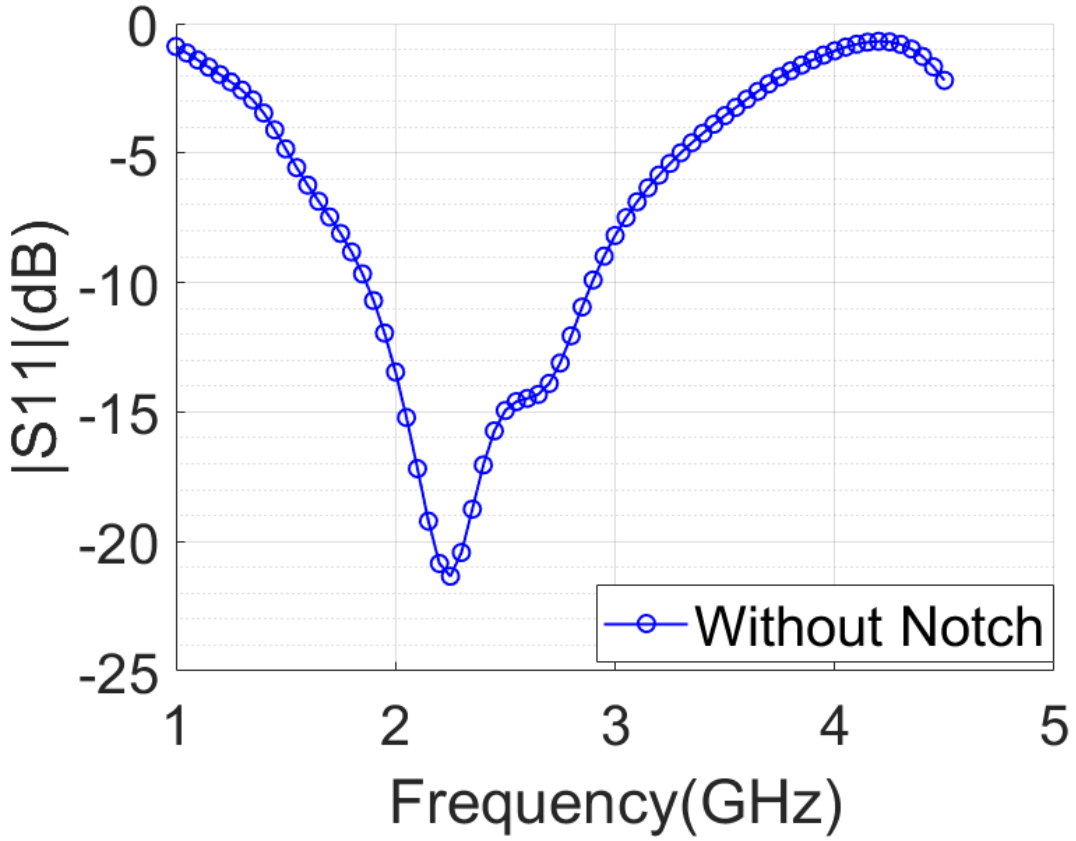

Figure 2. 9 Return loss graph of the antenna that does not contain notch

As can be seen from the Figure 2.9, antenna has a bandwidth of about 1 GHz. The results of the antenna design with one notch are given below. Figure 2.10 is used to prove that the surface current distribution is increased when the one notch is used.

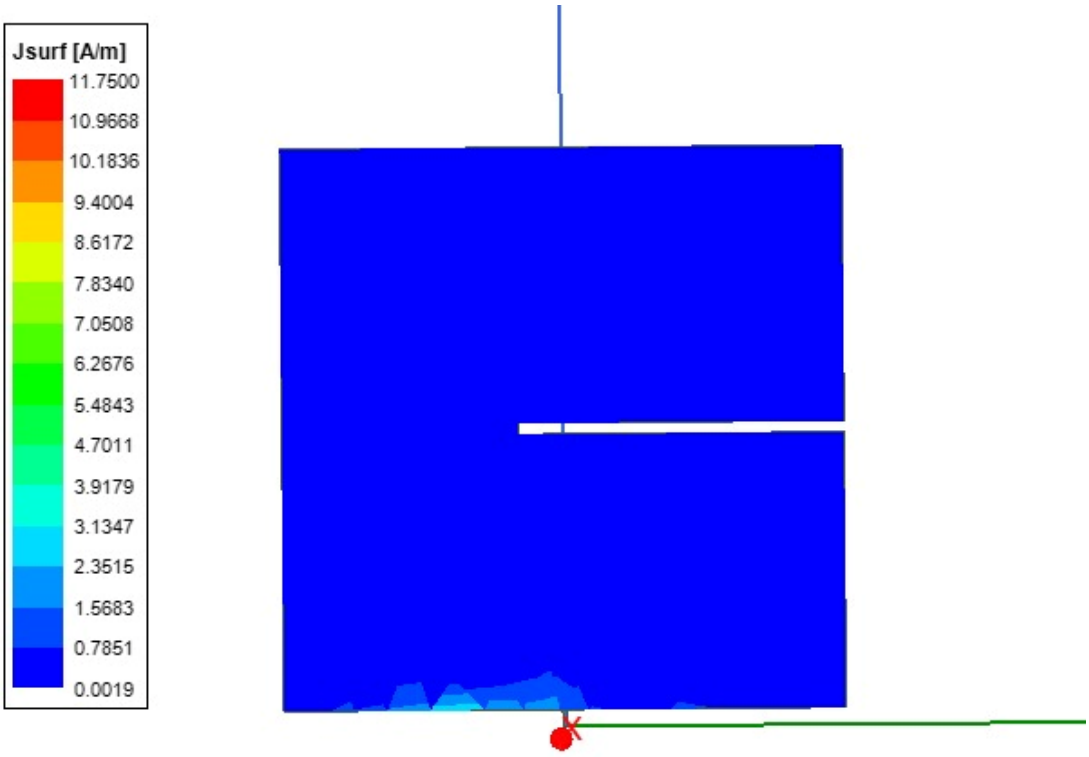

Figure 2. 10 The surface current distribution of the one notch

One can claim from the Figure 3.2 and 3.4, the surface current distribution is close to each other. Considering the notched antenna at these frequencies, the surface it is expected that the current distributions are concentrated in the notch regions. However, the surface current concentrated at the excitation area. Figure 3.11 is used to show the return loss graph of the 1-Notch square monopole antenna.

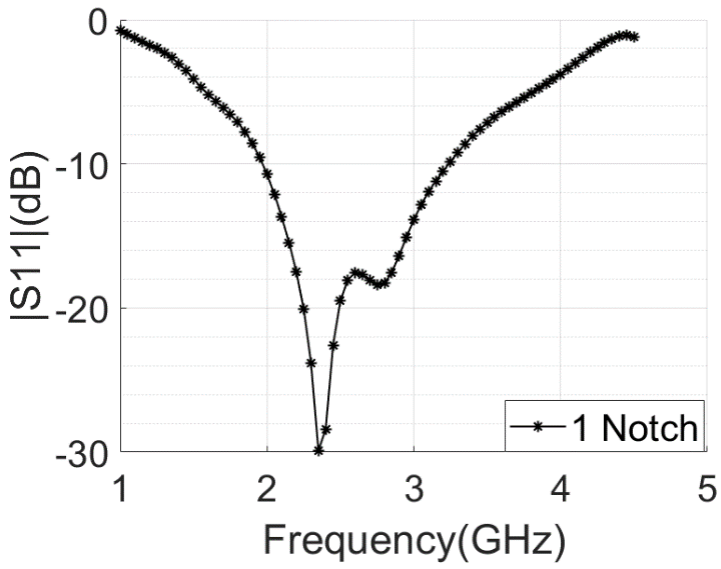

Figure 2. 11 The return loss graph of the 1-Notch square monopole antenna

As can be seen from the Figure 2.11, the gained bandwidth is 1.20 GHz. One can claim From Figure 2.9 and Figure 2.11, when one notch is used, the bandwidth is increased. Figure 2.12 is used to prove that the surface current distribution is increased when the two notch is used.

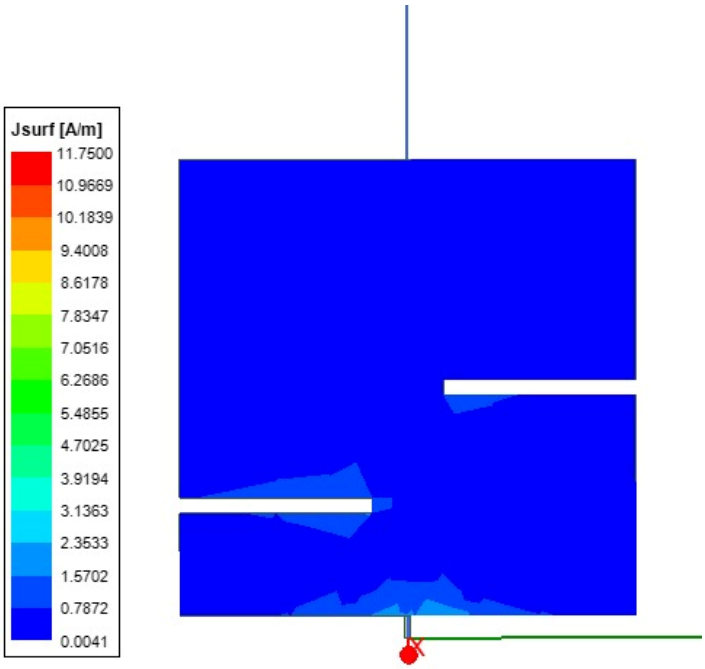

Figure 2. 12 The surface current distribution of the two notches

The current distributions are concentrated in the notch regions as can be seen from Figure 2.12. Figure 2.13 is used to show the return loss graph of the 2-Notch square monopole antenna.

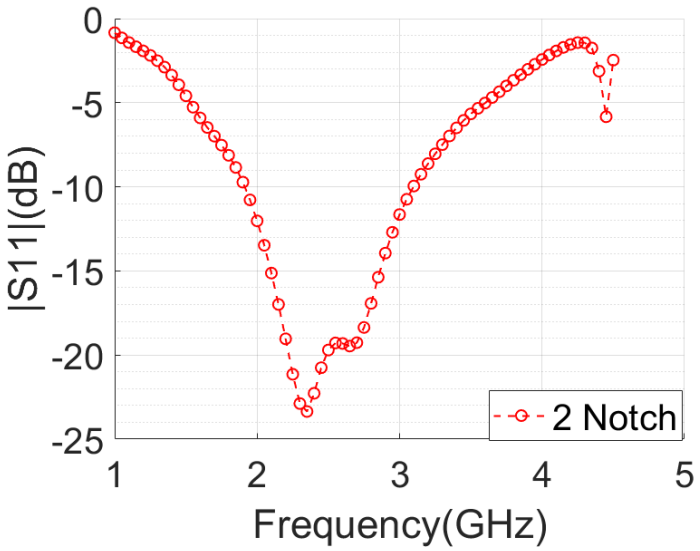

Figure 2. 13 The return loss graph of the 2-Notch square monopole antenna

One can claim from the Figure 3.7, the bandwidth is about 1.2 GHz like one notch antenna. Also, In addition, one more inference can be made about this situation, When the bandwidth does not increase, while adding more notch, the surface current distribution also does not increase.

The results of the antenna design with three notches are given below. Figure 2.14 is used to prove that the surface current distribution is increased when the three notch is used.

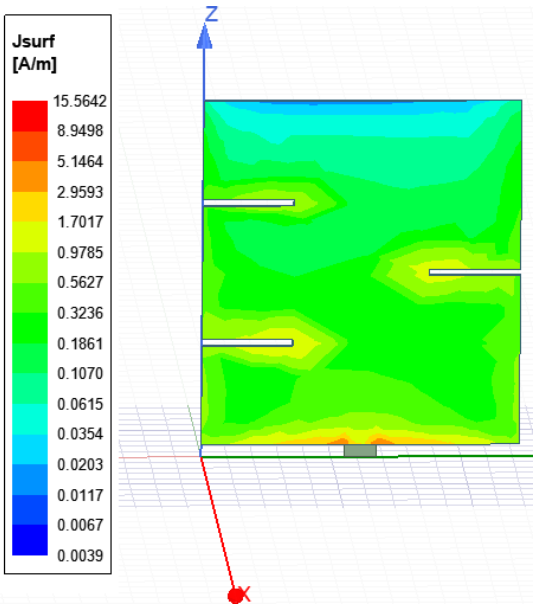

Figure 2. 14 The surface current distribution of the three notches

As can be seen from the Figure 2.14, the surface current distribution is showed best performance so far. Also, it can be seen from the same figure, J_{surf} value is increased

compared to 1-notch antenna and without notch antenna. Figure 2.15 is used to show the return loss graph of the 3-Notch square monopole antenna.

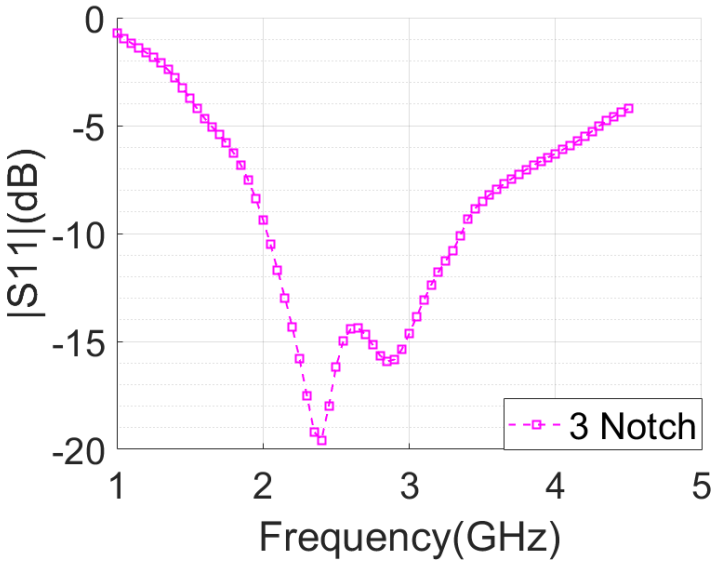

Figure 2. 15 The return loss graph of the 3-Notch square monopole antenna

Figure 2.15 shows that 3 notch antenna has the most wide band antenna so far. Also, the surface current distribution is also increased, simultaneously.

An antenna with 4 notches is obtained by increasing the number of notches is given below. Figure 2.16 is used to prove that the surface current distribution has a limit to increased. Because of that, the The antenna results are as follows,

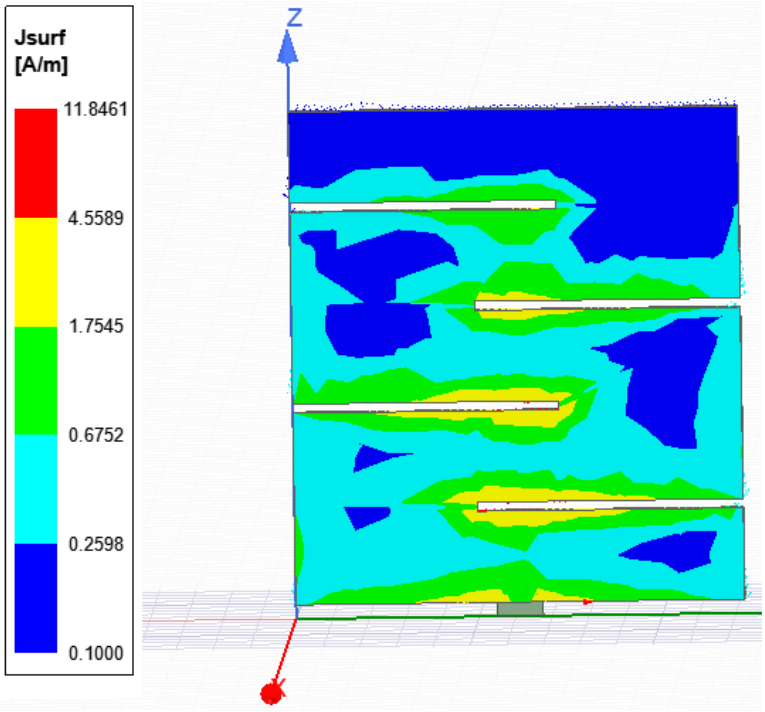

Figure 2. 16 Surface Current Distribution of the 4-Notch

One can state from the Figure 3.10, the surface current distribution is decreased when fourth notch is used. Figure 2.17 is used to show the return loss graph of the 4-Notch square monopole antenna.

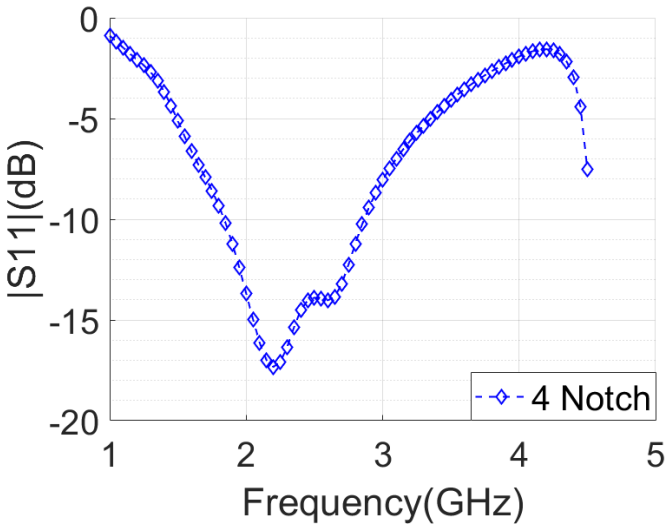

Figure 2. 17 Return loss graph of the 4-Notch square monopole antenna

As can be seen from the Figure 2.17, the bandwidth is decreased, when it is compared to 3 notch antenna. The 4-notch antenna has a bandwidth around 0.95 GHz. With the increase of the number of notches to four, when the results of the S parameter were examined, it was observed that the operating frequency decreased and shifted to the left. Also, the bandwidth is decreased. The antenna that does not contain a notch, 1-notch, 2- notch, 3- notch, 4- notch antenna S_{11} result shown below Figure 2.18.

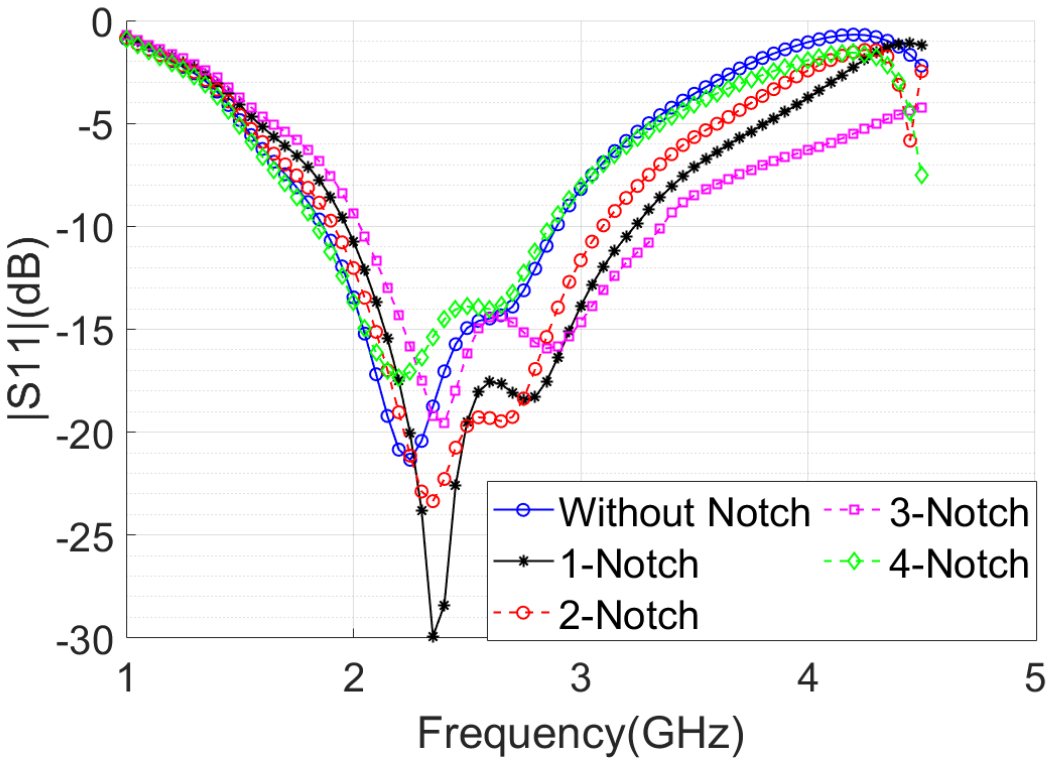

Figure 2. 18 Comparison of Notched Square Monopole Antenna

It can be said that the antenna shows the best performance when it has three notches. To make it clear, three notch antenna has more wideband to other antennas. Having a more surface current distribution also mean antenna has more efficient than other antennas. Because of that, three notch antenna is selected to apply ANN.

2.3. Effects of Antenna Design Parameters on S_{11}

In this subsection, it is aimed to reveal how S_{11}(dB) changes by changing the length and width of the notches and other parameters on the antenna designed in Figure 2.7. In the simulations, the variation of the S_{11} parameter was observed by considering different measurements for each length shown in Figure 2.19. In parametric analyzes, firstly, analyzes related to antenna length, which is the most key factor in frequency tuning of the antenna, were made.

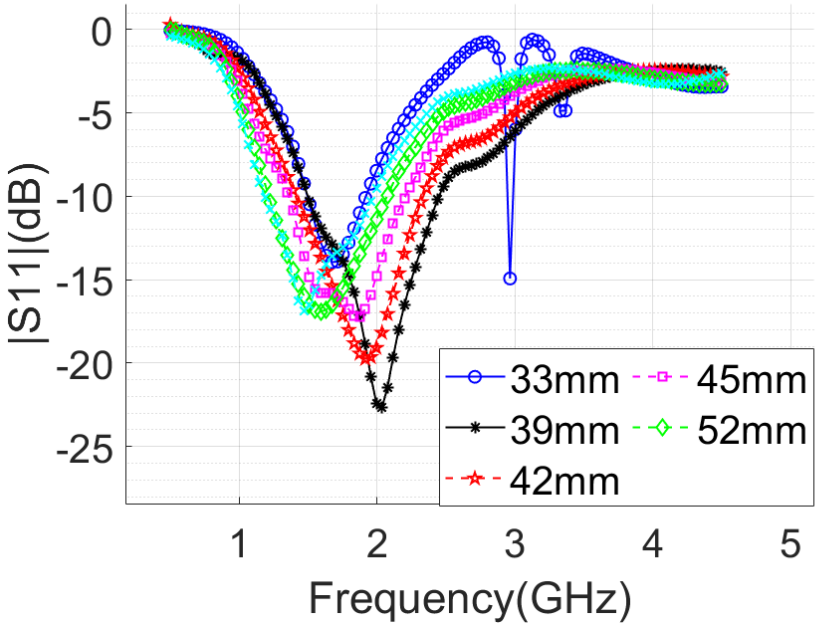

Figure 2. 19 Comparison of Notched Square Monopole Antenna

The variation of the "Length" parameter of the antenna shown in Figure 2.19 has been observed in how the S11 parameter changes at 33 mm, 39 mm, 42 mm, 52 mm lengths with 6 mm intervals. The results of the simulation study are given in the graph in Figure 2.19. It can be seen from the Figure 2.19, if the length is increase, the frequency is decreased. Figure 2.21 and Figure 2.20 is used to show effect of notch width and notch length on antenna, respectively.

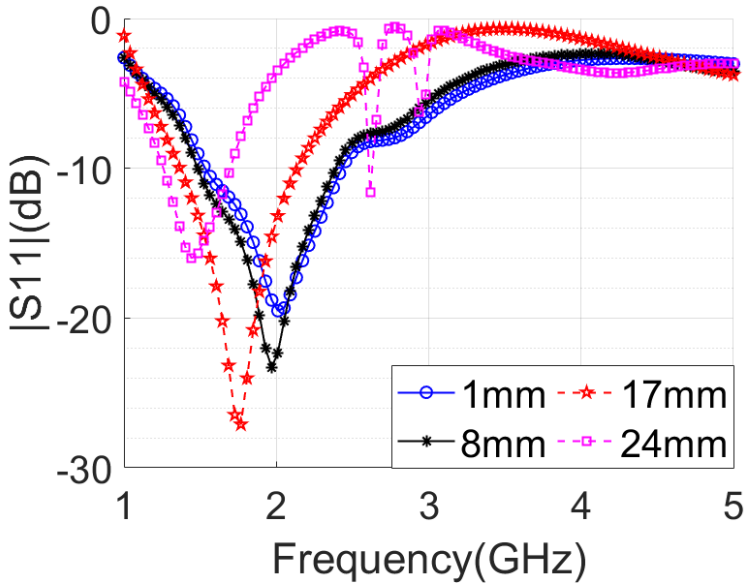

Figure 2. 20 Effect of Notch Length on S_{11}

The variation of the "Notch Length" parameter of the antenna shown in Figure 3.1 has been observed in how the S_{11} parameter changes at 1 mm, 8 mm, 17 mm, 24 mm lengths with 7 mm intervals. The results of the simulation study are given in the graph in Figure 2.21. Also, one can state from Figure 2.20, Notch length can be used to tune the antenna operating frequency. It can be seen from the Figure 2.19, if the notch length is increase, the frequency is decreased. Moreover, antenna length is the most important to tune the antenna operating frequency.

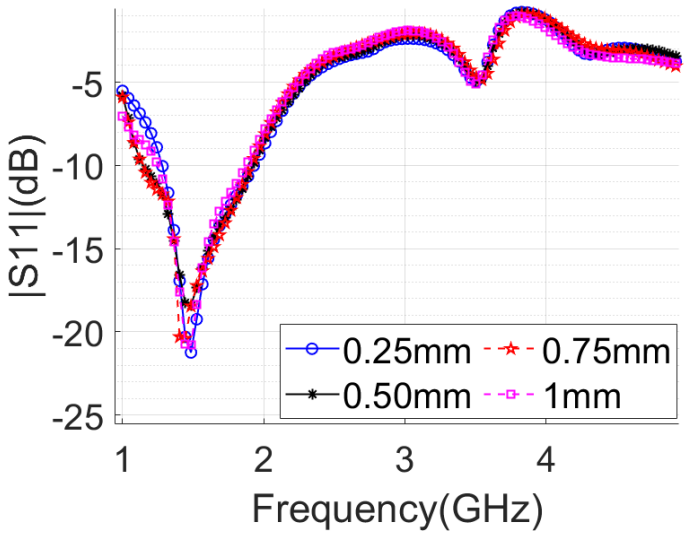

Figure 2. 21 Effect of Notch Width on S_{11}

The variation of the "Notch Width" parameter of the antenna shown in Figure 3.1 has been observed in how the S_{11} parameter changes at 0.25 mm, 0.5 mm, 0.75 mm, 1 mm widths with 0.25 mm intervals. The results of the simulation study are given in the graph in Figure 2.21. One can claim from Figure 3.16, Notch width is significant on antenna matching performance, it can be used to have a better return loss value. Notch width is not suitable to tune the antenna operating frequency. Only the width of the ground plane (W) is altered in this section of the study; all other antenna design parameters remain unchanged. Figure 2.22 shows the effect of ground plane width on S_{11}.

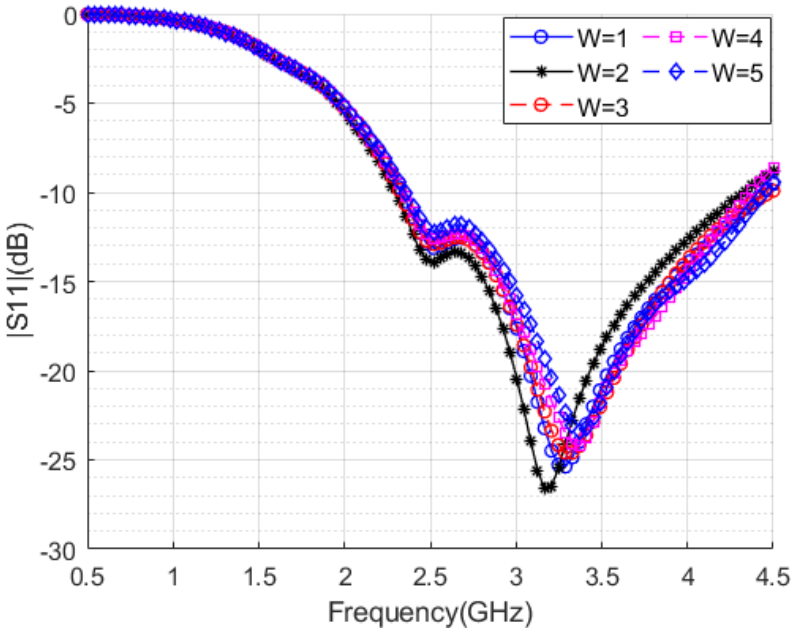

Figure 2. 22 Effect of Ground plane Width on S11

It is seen that as W changes, resonant frequency does no change dramatically. This section uses a parametric analysis to examine how ground plane length (S) affects resonant frequency. Figure 2.23 shows the effect of ground plane length on S_{11}.

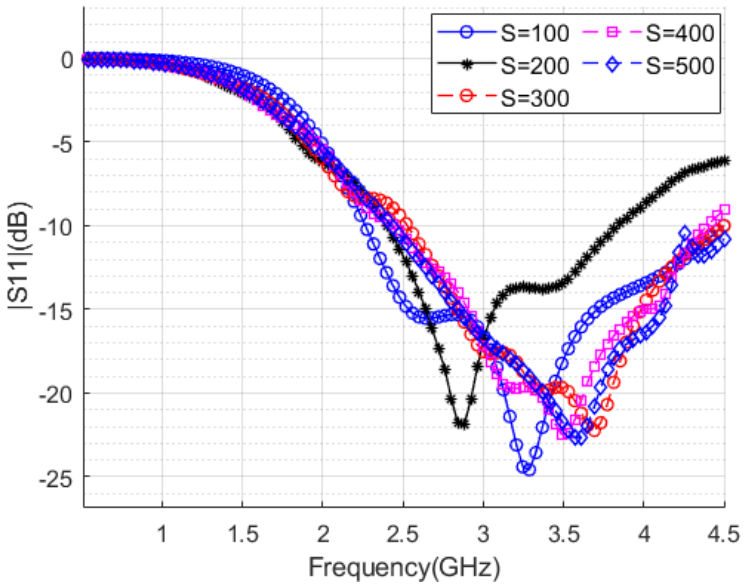

Figure 2. 23 Effect of Ground Plane Length on S11

It is seen that as W changes, resonant frequency does no change dramatically. The impedance bandwidth of an antenna is also influenced by the radiator thickness. In order to

see this effect, WA is increased in 0.5 mm increments from 0.5 to 2.5 mm. Figure 2.24 shows effect of thickness of radiator on S_{11}.

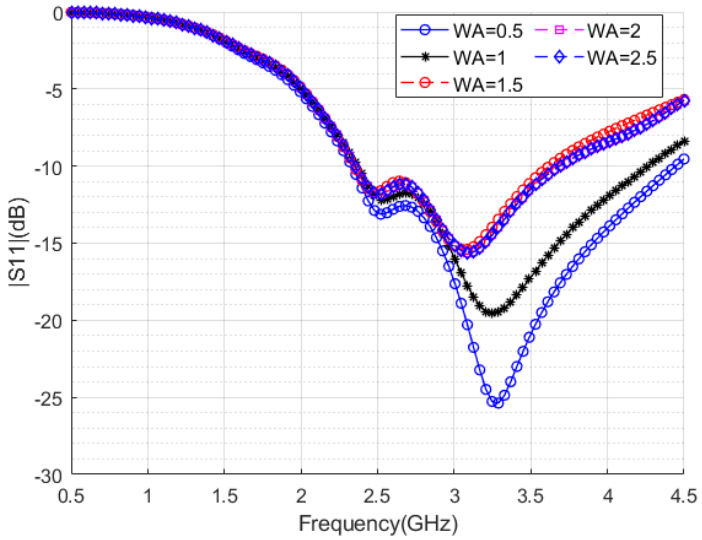

Figure 2. 24 Effect of Thickness of Radiator on S_{11}

As seen, the best variation is when WA equals to 0.5. The monopole radiator to ground plane gap (h) has an impact on the antenna's impedance bandwidth. Only the gap (h) is altered in this section of the study. The antenna's other characteristics stay constant. For gap lengths of 0.5 mm, 1 mm, 1.5 mm, 2 mm, and 2.8 mm, S_{11} is presented in Figure 2.25.

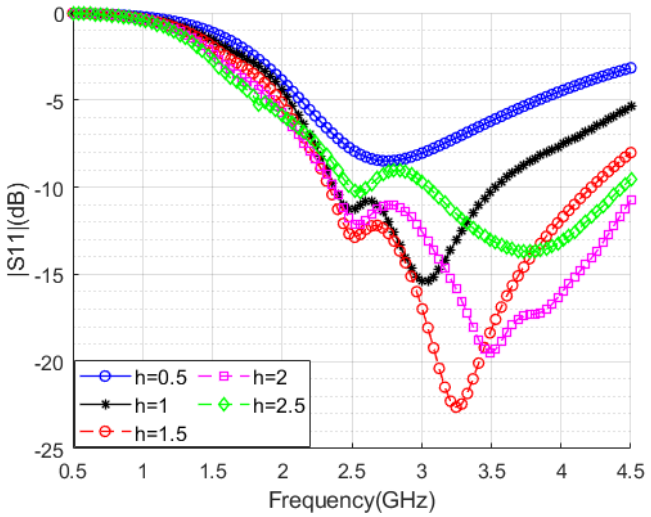

Figure 2. 25 Effect of the gap (d) between monopole patch and ground plane on S11

3. Artificial Neural Network

Artificial neural networks are likened to the human brain. Since these neural networks are connected to the central management system, they form a network. That is why it is called a neural network [28].

3.1. Introduction to ANN

The advantages of a neural network-based approach over previous approaches include adaptive learning, distributed association, non-linear mapping, and the ability to manage inaccurate inputs [29]. A neural network model can be trained to respond to unknown factors using prior measurement data, according to literature searches [29]. In this paper, this specification of ANN is evaluated by unknown variables. ANN has been successfully used to simulate nonlinear systems. Training datasets can sometimes reveal patterns that are independent of mathematical models. When similar patterns are observed, ANNs return a result with the lowest mean-squared error [30]. The input vector is transformed by the ANN into the appropriate output vector. No additional values are needed. As a result, ANNs are extremely efficient at simulating nonlinear links without using pre-existing models [31].

3.2. ANN Training Algorithms

The LM, SCG, and BR feedforward backpropagation algorithms power the suggested antenna. Data in feedforward networks moves from input to output in a single direction. The algorithmic strategies of ANN in the literature include adaptable momentum (ADP), self-adaptive learning rate (SLR), resilient backpropagation (RB), conjugate gradient (CG), quasi-newton, and Bayesian regularization (BR) [36]. The data processing speed, memory footprint, and precise performance of these algorithms are differentiated. By computing the root mean square error and simulating data learned in electromagnetic (EM) design programs like HFSS, one may determine how well the approach performs. This article compares the efficiency of LM, SCG, and BR in terms of MSE and EM result correctness. The performance of the ANN is needed. The performance criterion is mean square error that calculated as (3.1) [36],

$$MSE = \frac{1}{m_1 \cdot q_{\text{out}}} \sum_{m=1}^{m_1} \sum_{k=1}^{q_{\text{out}}} e_k^2(m) \tag{3.1}$$

As seen, for all pattern in the ANN, the error $e_k^2(m)$ of the k^{th} neuron in the output layer for the m^{th} pattern is calculated. The accuracy of the algorithm is based on the correlation between the output obtained by evaluating the antenna parameters trained in the EM design program and the neural network output values of the antenna parameters that were calculated. The figure shows the three layers of the Perceptron Network (MLP), which consists of more than one hidden layer.

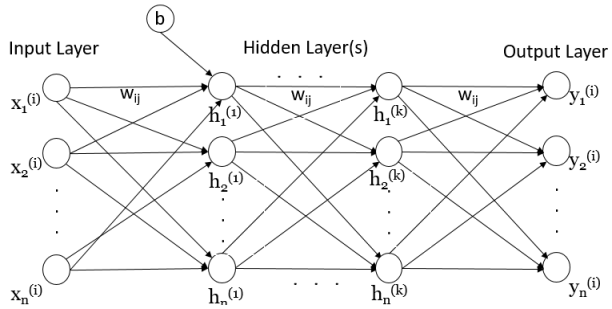

Figure 3. 1 Multilayer Perceptron ANN

The input quantities, the neurons which are in hidden layer and the output variables are denoted as $x_{(n)}^{(i)}$, $h_{(n)}^{(k)}$ and $y_{(n)}^{(i)}$ respectively. In this study, input layer has two quantities to train the neural network whereas the output layer has three antenna design variables. Thus, number of the input and the output is independent from each other. Mathematically, the neuron named as $h_{(n)}^{(k)}$ which is in the hidden layer transfers input quantity by multiplying weight and bias. The MLP operation can be summarized as [37],

$$\begin{aligned} h_i^{(1)} &= \phi^{(1)}\left(\sum_j w_{ij}^{(1)} x_j + b_i^{(1)}\right) \\ h_i^{(\mathrm{n})} &= \phi^{(\mathrm{n})}\left(\sum_j w_{ij}^{(\mathrm{n})} h_j^{(\mathrm{n}-1)} + b_i^{(\mathrm{n})}\right) \end{aligned} \tag{3.2}$$

$$y_n^{(\mathrm{i})} = \phi^{(3)}\left(\sum_j w_{ij}^{(3)} h_j^{(2)} + b_i^{(3)}\right) \tag{3.3}$$

Where, φ is the nonlinear activation function.

3.3. Description of the Levenberg-Marquardt algorithm

The LM algorithm [40] is a change in the Gauss-Newton confidence region [42]. The most major step in this calculation is to calculate the Jacobian network. For the neural organization mapping problem, the terms within the Jacobian network can be computed by adapting a backpropagation algorithm [43]. The Levenberg-Marquardt algorithm can approximate the second order preparation rate without needing to calculate the Hessian lattice. This approximation can be achieved by using [38].

$$H = J^T J \tag{3.4}$$

Also, the gradient can be written as [38]:

$$g = J^T e \tag{3.5}$$

Where J is the Jacobian matrix and e is vector of network errors.

The Levenberg-Marquardt algorithm uses the equation below that approximates a Hessian Matrix [38]:

$$x_{k-1} = \mathbf{x}k - [J^T J + \mu I]^{-1} \text{J}^{'} \text{e} \tag{3.6}$$

3.4. Description of the Bayesian regularization backpropagation algorithm

Bayes' theorem is a conditional probability that can be used to make inverse predictions [33,34]. The Bayesian regularization algorithm is a minimization calculus that seeks to minimize a direct combination of squared errors and weights [35,36]. It also strives to improve the generalization of the qualities of the network by modifying its direct combination. These processes are performed in the Levenberg-Marquardt algorithm. Briefly, BR is a learning algorithm that utilizes an optimization algorithm which is linear in order to refresh weights and bias values. The right combination of squared errors and weights can be used to build a network that generalizes well. Minimizing a combination of squared errors and weights is the best way to achieve this goal. Yue, Songzheng and Tianshi describe how BR includes network weights that are updated in the training objective function given by function of F notated as, F(w) in (3.7) [32].

$$F(\omega) = \alpha E_\omega + \beta E_D \tag{3.7}$$

The error-distribution function, E_w, is the sum of the network errors and the squared network weights. α and β are the parameters of the objective function. Bayes' theorem provides a way to calculate the relative importance of two factors. α and β. As shown in

(3.8), A and B is connected by their prior which is also called as marginal and subsequent which also called as conditional. This operation made in Bayes' theorem [33,34].

$$P(A \mid B) = \frac{P(B \mid A)P\ A)}{P(\ B\ )} \tag{3.8}$$

As seen, the posterior probability of conditional A on B is P (A | B) and the a priori probability of conditional B on A is P (B | A). The non-zero probability of previous event B serves as a normalization constant. To find the best weight space, you must reduce the target function to find its best value. This is like maximizing the posterior probability function, which is explained in (3.9).

$$P(\alpha, \beta \mid D, M) = \frac{P(D \mid \alpha, \beta, M)P(\alpha, \beta \mid M)}{P(D \mid M)} \tag{3.9}$$

Where P (D | M) is the normalization factor, P (D | M) is the uniform a priori density for the regularization parameters, and P (D | α, β, M) is for the probability function of D for given α, β, M. Where D is the weight distribution and M is the unique architecture of the neural network. The probability function P (D | α, β, M) is identical to maximizing the posterior function P (α, β, | D, M). With the use of this method, ideal values for are found for a specific weight space. The method then moves on to the LM phase, which involves updating the weight space and computing the Hessian matrix in order to minimize the objective function. When convergence is not attained, the method guesses fresh values for and keeps trying until it is [32].

3.5. Description of the Scaled Conjugate Gradient Backpropagation Algorithm

LM and the SCG differ has minor difference. This distinction can be explained by the fact that SCG is frequently utilized in low memory situations. Using the basic backpropagation method, the weights are dumped in the direction of descent with the steepest slope, i.e., H the highest negative gradient. The power function's fastest decreasing direction is in this direction. It turns out that the fastest convergence does not always occur when the function lowers the most along the gradient's minus side [34]. The conjugate gradient algorithms seek a path that, while maintaining the error reduction attained in the preceding path, typically delivers a faster convergence than the steepest descent direction. All CG algorithms begin their initial search in the steepest descent direction (3.10) [45]. CG

algorithms are frequently used in row search. In other words, the step size is determined using a linear search strategy rather than using Hessian matrix approximation (3.11). The following direction of search is then chosen so that it is conjugated with the preceding direction (3.12). The following direction of search is then chosen so that it is conjugated with the preceding direction (3.12).

$$p_o = -g_0 \tag{3.10}$$

$$x_{k+1} = x_k + \alpha_k g_k \tag{3.11}$$

$$p_k = -g_k + \beta_k p_{k-1} \tag{3.12}$$

The various CG algorithms are differentiated by how the factor is computed. A technique other than the line search methodology can be used to estimate the step size. The model trust region strategy used by LM algorithms and the CG methodology will be combined. This technique is known as the SCG approach, and Moller [46] is credited with first introducing it to the literature.

In this technique which is donated as the Hessian matrix approximation. λ_k and σ_k are the scaling factors to are utilized to approximate Hessian matrix. These scaling factors are initialized by the user at the beginning of the process so that $0< \lambda_k <10\text{-}4$ and $0< \sigma_k <10\text{-}4$. For SCG, the βk factor and new search direction may be given as follows: (Section 3.13, 3.14, and 3.15. He was completely stunned. I woke him up, like, five minutes ago. According to [46]

In this method, Hessian matrix is estimated as scaling factors are combined to each other. Moller [46], explained each step to approximate Hessian matrix as,

$$s_k = \frac{E'(w_k + \sigma_k p_k) - E'(w_k)}{\sigma_k} + \lambda_k p_k \tag{3.13}$$

$$\beta_k = \frac{(|g_{k+1}|^2 - g_{k+1}^T g_k)}{g_k^T g_k} \tag{3.14}$$

$$p_{k+1} = -g_{k+1} + \beta_k p_k \tag{3.15}$$

4. Building ANN For the Metal-Plate Planar Monopole Antenna

The related ANN model in this work focuses on estimating antenna dimensions as a function of resonant frequency and bandwidth whereas the corresponding ANN models in earlier studies, which may be defined as finding the resonance frequency as a function of geometric structure. In order to obtain, training set of ANN, EM simulations are carried out for the different value of physical dimensions. These physical dimensions also called as target values. Target values are created from the physical dimensions of the antenna are built according to previous work [18]. The Target values are L, NL and NW. NL and NW are procured from 1mm to 24mm with linear step of 2mm, from 0.25mm to 1.25mm step of 0.25mm, respectively. L is manufactured is manufactured from 25mm to 59mm with linear step of 2mm. The length L is chosen so that the antenna covers the L & S bands. The NL length was chosen to reach the far end of the antenna. The NW length was chosen to avoid EM analyzes being too long. These variables were transferred to the EM simulation and analyzed. This operation is called as parametric analysis. The parametric analysis two points are emphasized: one is the center of the antenna working frequency spectrum and other is the fractional bandwidth of the modelled antenna.

Center of the antenna working frequency spectrum and fractional bandwidth is named as f_c and BW. f_c and BW are the input variables of the synthesis stage. The range of these target values initially set as Table 1.

Table 1 Initial range of target values

Variable	Start	Stop	Step
L	25(mm)	59(mm)	1(mm)
NW	0.25(mm)	1.25(mm)	0.25(mm)
NL	1(mm)	24(mm)	2(mm)

With these target values, result of EM simulations show that unexpected abrupt changes occurred at center frequency and bandwidth. Therefore, target set should be reorganized with respect to obtain expected frequency and bandwidth results. In order to obtain this, curve fitting algorithm is utilized for EM simulation results. The Curve fitting is done by using polynomial fitting method. As can be seen from the Figure 4.1, the target values are L, NL and NW as named, antenna length, notch length, notch width, respectively whereas input variables are f_c and BW

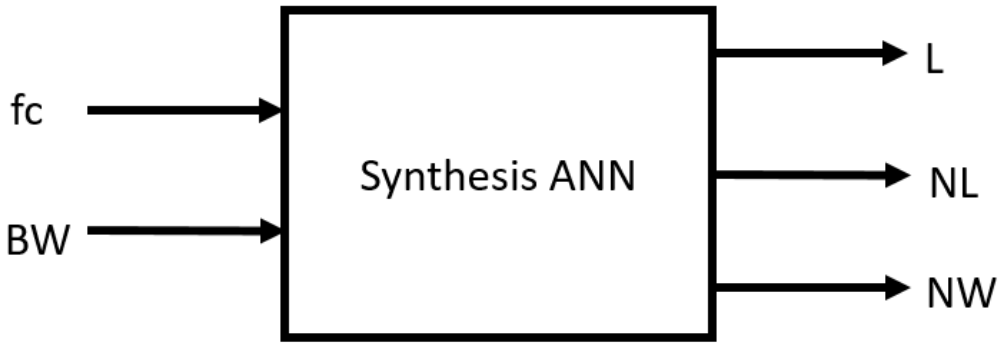

Figure 4. 1 Synthesis stage of the ANN

These target values are curve fitted with respect to input values f_c (center of operating frequency) and BW (bandwidth). Table 2 shows range of target values after curve fitting.

Table 2 Range of target values after curve fitting.

Variable	Start	Stop	Step
L	25(mm)	59(mm)	1(mm)
NW	0.25(mm)	1.25(mm)	0.25(mm)
NL	1(mm)	17(mm)	2(mm)

These range of target values are utilized at EM simulations in order to obtain training set of ANN. Training set consists of fc and BW as an input values, L, NL and NW as a target values. The size of the initial training set is 1164 different input and target values. The example of training set is given in Table 3.

Table 3 Example training set.

Input Training Data		Target Training Data		
fc	**BW**	**L**	**NL**	**NW**
1.80	44.4	41(mm)	15(mm)	1(mm)
1.40	50	47(mm)	23(mm)	1.5(mm)
1.99	44.2	35(mm)	15(mm)	1.25(mm)

The training set includes center of frequency and bandwidth to corresponding length(L), notch length (NL) and notch width(NW) as shown in Figure 4.2 below.

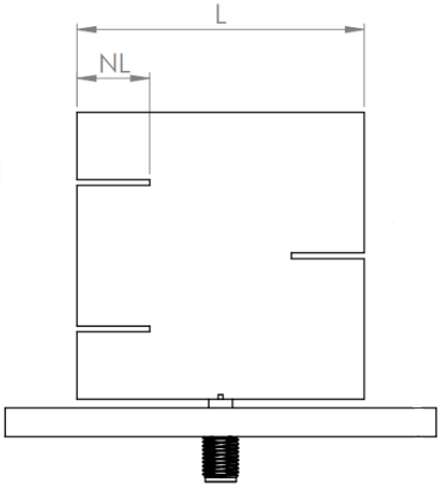

Figure 4. 2 Training Data Set Variables

In order to verify operation of ANN, analysis should be done in the reverse form of the synthesize operation. This can be called as analysis stage of the ANN. Analysis stage of the ANN can be seen from Figure 4.3.

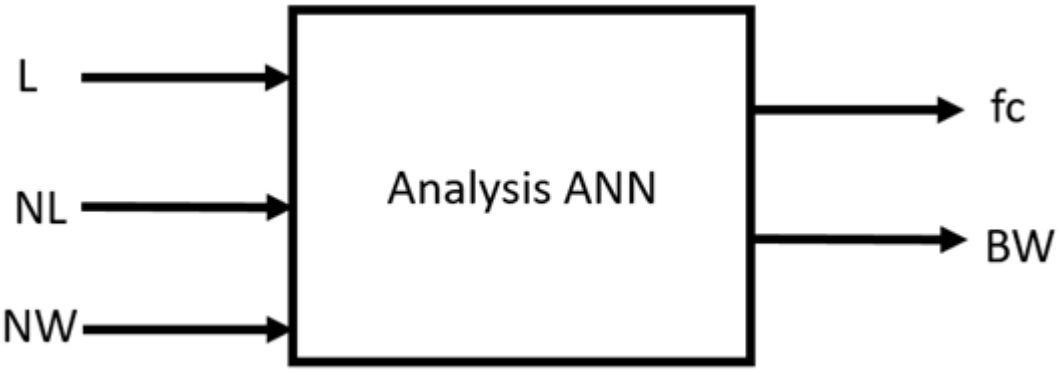

Figure 4. 3 Analysis stage of the ANN

Since, distinct antenna design parameters give the same f_c and BW rarely, the dataset is chosen by considering the antenna efficiency. The data from the training set is separated into three sections in our analysis: 70 percent is utilized for training, and 15 percent is used for testing and validation, respectively. This setup is also used in analysis stage. ANN prediction accuracy is evaluated a new set that only contains f_c and BW values. This dataset can be called as test dataset. Test dataset is created randomly from the minimum value to maximum value of f_c and BW. The test dataset's input variables are notated as fc' and BW', the output of the ANN predicted variables are named as L'', NL'', NW''. The output of the EM simulations named as f_c-EM and BW-EM. Table 4 shows the EM results of the simulated ANN values of the Antenna.

Table 4 The EM results of the simulated ANN values of the Antenna

L''	NL''	NW''	f_c - EM	f_c'	BW- EM	BW'
41.17	8.32	0.74	1.934	1.927	48	47.58
42.86	10.59	0.70	1.853	1.820	50.1	47.60
49.50	11.12	0.73	1.651	1.633	46.5	49.92
37.50	8.34	0.71	2.156	2.235	49	49.1
24.17	3.66	0.80	3.408	3.429	62	61.3
22.89	1.71	0.84	3.549	3.588	64	64.2

The fractional bandwidth BW is calculated as follows [1]:

$$BW = \frac{f_h - f_L}{f_c} x100\% \tag{4.1}$$

Where f_h is the operation band's higher frequency, f_L is the operating band's lower frequency.

In Table 5, output of the analysis ANN values is compared to each algorithm in terms of accuracy. The accuracy is computed for each training algorithm. Accuracy is computed as (4.2),

$$fc - \text{Accuracy} = \frac{\text{fc} - \text{ANN}}{\text{fc} - \text{Target}} x100\%$$
$$BW - \text{Accuracy} = \frac{\text{BW} - \text{ANN}}{\text{BW} - \text{Target}} x100\% \tag{4.2}$$

Table 5 Accuracy comparison of each algorithm.

Algorithm	f_c - Accuracy	BW – Accuracy
LM	99	98
SCG	93.91	96.72
BR	93.89	93.77

One can state that from Table 5, LM has the best accuracy performance among other algorithms. Because of that, LM is chosen to apply trained dataset to EM design program. The output of the LM algorithm is simulated in EM design program HFSS.

The accuracy is 99% for fc and 98% for BW. It can be said that the LM algorithm performs quite well when compared to the target values in the EM simulation results. Table 6 shows the performance of ANN when it is applied to out-of-band. In other words, a new test dataset is used to check ANN performance on not trained dataset. Although, as mentioned before the ANN is trained by L-band and S-band data, C-band and UHF-band frequency spectrum is evaluated by the ANN. The dataset of C-band and UHF-band input values are created randomly by MATLAB.

Table 6 The out of band EM results of the simulated ANN values of the antenna

L*	**NL***	**NW***	**f_c***	**BW***	**f_c – EM Accuracy**	**BW% - EM Accuracy**
18.95	6.06	0.7	4.1	55%	95%	96%
59.8188	35.93	0.25	0.8	23%	71%	65%

f_c* and BW* are the testing datasets to produce ANN output variables which are L*, NL* and NW*. The testing datasets are produced to show performance of ANN in C-band and UHF-band. The ANN variables are simulated in EM design program HFSS. Then the accuracy is calculated. One can claim that, in C-band ANN is successful because of having a high accuracy whereas in UHF-band the accuracy is low comparatively low. S11 graph of the ANN output simulations of HFSS is given in Figure 4.4.

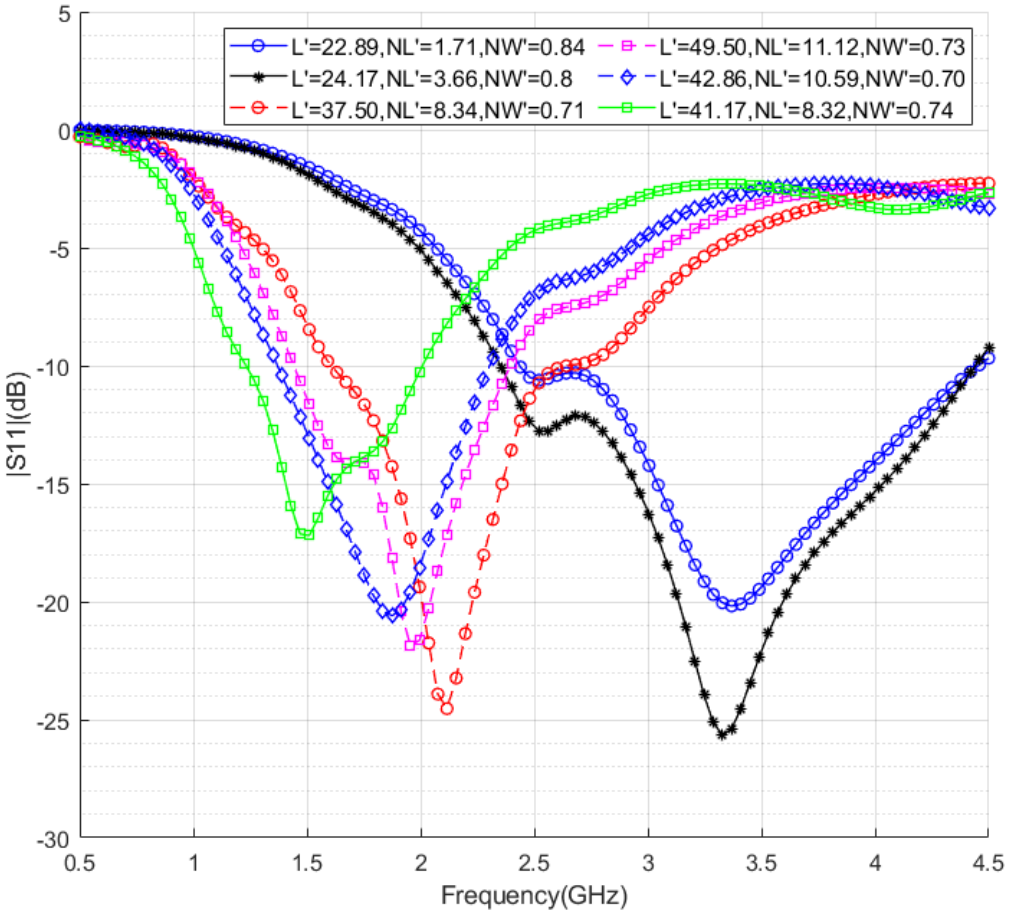

Figure 4. 4 EM Simulation Results of the Values Created By ANN

For L'=22.89, NL'=1.71, NW'= 0.84 the predicted fc and BW equal to 1.927, 47.58, respectively. As seen, fc and BW equal to 1.934 and 48, respectively. One can claim the EM simulation result and desired values are close to each other. Because of that the ANN system is successful to predict the antenna. Out of band test of the ANN is also simulated in EM environment. The ANN created antenna geometry to apply EM simulation. The Figure 4.5 shows the out of band test outputs of the ANN.

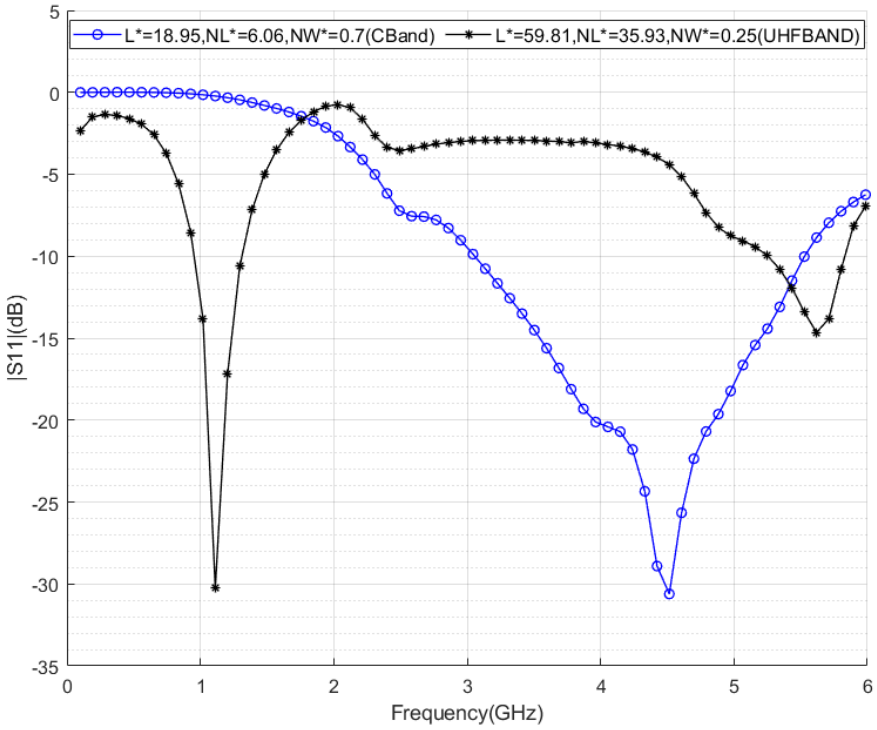

Figure 4. 5 EM Simulation Results of the Out of Band Dataset

One can claim from Figure 4.5 and Table 6, the prediction performance decreases when the training data set digress from demanded antenna operating frequency band. As can be seen from the Figure 4.5, the antenna's bandwidth is become narrower when the frequency decreases. C band antenna has wider bandwidth than UHF band antenna. The prediction performance of C band is more successful than UHF band antenna because the accuracy of C band antenna equals to %ninety-six whereas UHF band antenna's accuracy equal to %sixty-five.

4.1. ANN Results with Respect to MSE and Regression

The neural network learns input data patterns by reading the dataset and doing various computations on it. But the neural network does not learn once; it learns again and over again, utilizing the input dataset and past trial outcomes this situation leads to proses more epoch. Because of that, the ANN processing step takes a lot of times. An epoch is a unit of time used to learn from the input dataset. An epoch is a single loop across the whole training dataset. Training a neural network usually takes many epochs. Increasing the number of epochs does not automatically imply better outcomes from the network. So, via trial and error, we select many epochs where the findings remain consistent after a few cycles. Numerous iterations are done to reach full epoch. The number of batches or steps

through partitioned packets of training data required to complete one epoch is called iteration. Design goals and design parameters of the proposed ANN are given at Table 8.

Table 7 ANN desing parameters and their values

Parameter	Value	Description
Epochs	1000	Maximum number of epochs to train
Max_Fail	6	Maximum validation failures
Min_grad	$1e^{-7}$	Minimum performance gradient
mu	0.001	Initial Mu
Mu_dec	0.1	Mu decrease factor
Mu_inc	10	Mu increase factor
Mu_max	$10e^{10}$	Maximum Mu

To have more accurate and have shorter ANN session, the input and target variables are fitted to each other. This application made neural network is more accurate. To show the performance of the neural network system, the Figure 4.10 shows the before of the fitting application and Figure 4.11 shows the result of the fitting application. To understand the difference of the figures other terms about ANN is determined.

Regression is yet another key concept in ANN. To determine the strength and nature of a relationship between one dependent variable and a group of other variables, regression is a statistical approach that is used in finance, investing, and other industries (known as independent variables).

The hidden neuron is also significant to affect the neural network. Eight hidden neuron numbers are picked for this project. This number of hidden neurons is determined by many trials. The optimum hidden layer is selected when MSE is low at less epoch. R-values are used between the estimated output and actual output in the training, testing, and validation data to determine the number of nodes in the hidden layer.

The input layer has two design parameters, a hidden layer with eighth hidden nodes, and a two-node output layer for figure of merit. The R-value refers to the coefficient of correlation, which is a statistic that describes the strength of a link between two variables. R-value's formula may be given as follows (4.3) [33].

$$R = \frac{n\sum y_1 y_2 - (\sum y_1)(\sum y_2)}{\sqrt{n(\sum y_1^2) - (\sum y_1)^2}\sqrt{n(\sum y_2^2) - (\sum y_2)^2}} \quad (4.3)$$

The number of data pairs is denoted by the letter n. By varying the number of hidden layer nodes from 2 to 15, one may evaluate R-value for training, testing, and validation using the entire data set. The model with eight hidden nodes has the greatest R- value for training, testing, and validation. The results achieved when eight hidden nodes were employed for this ANN model are shown in Figure 4.10 Training, Testing, and Validation Plots of ANN fit. These are the charts that show the ANN-estimated outputs (network output) in relation to the output values in the training, validation, and test sets (target output). The data must align along a 45-degree line to be deemed a perfect fit, which indicates that the network outputs are equal to the objectives. As can be seen in Figure 4.10, the fit is reasonable for all data sets, with R values of 0.99 or above in each case. If this fit were not good enough, we could retrain the network using the 'Retrain' button in the neural network toolbox. The output predicted by the fitted-ANN model is shown by the vertical axis in each panel of Figure 5.7, while the real output value is represented by the horizontal axis. The four panels in this picture, starting from the top-left, correspond to training data, validation data, all data combined, and testing data, respectively. If the fit line in any of these plots is near to the 45^o line, the predictions for the related data are more accurate.

The ideal outcomes are shown by the dashed line, while the best fit of the output is represented by the solid line. The computed R value reflects the connection between the ideal fit and the network output. As shown in Figure 4.10, the value is near to one, indicating that the network is well-trained, and the amount of error is close to zero.

To get better performance, at the Synthesis stage, the input dataset is also fitted. As a result of this operation, obtained R value is approached one.

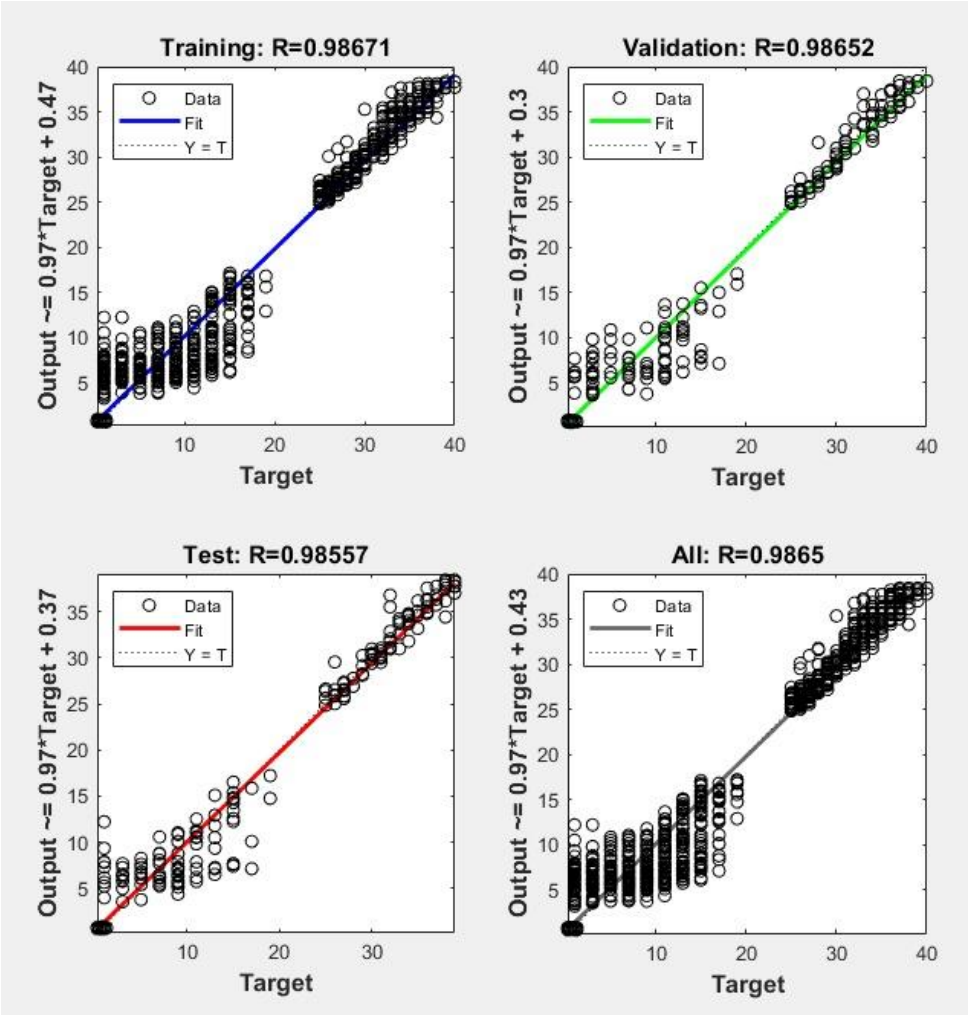

Figure 4. 6 Regression graph of Training, Validation and Test parts

As seen, before the curve fitting, some variables are far from the slope. This situation lowers the R-value. As can be seen at Figure 4.7, the fitting application helped to get R value is came closer to one.

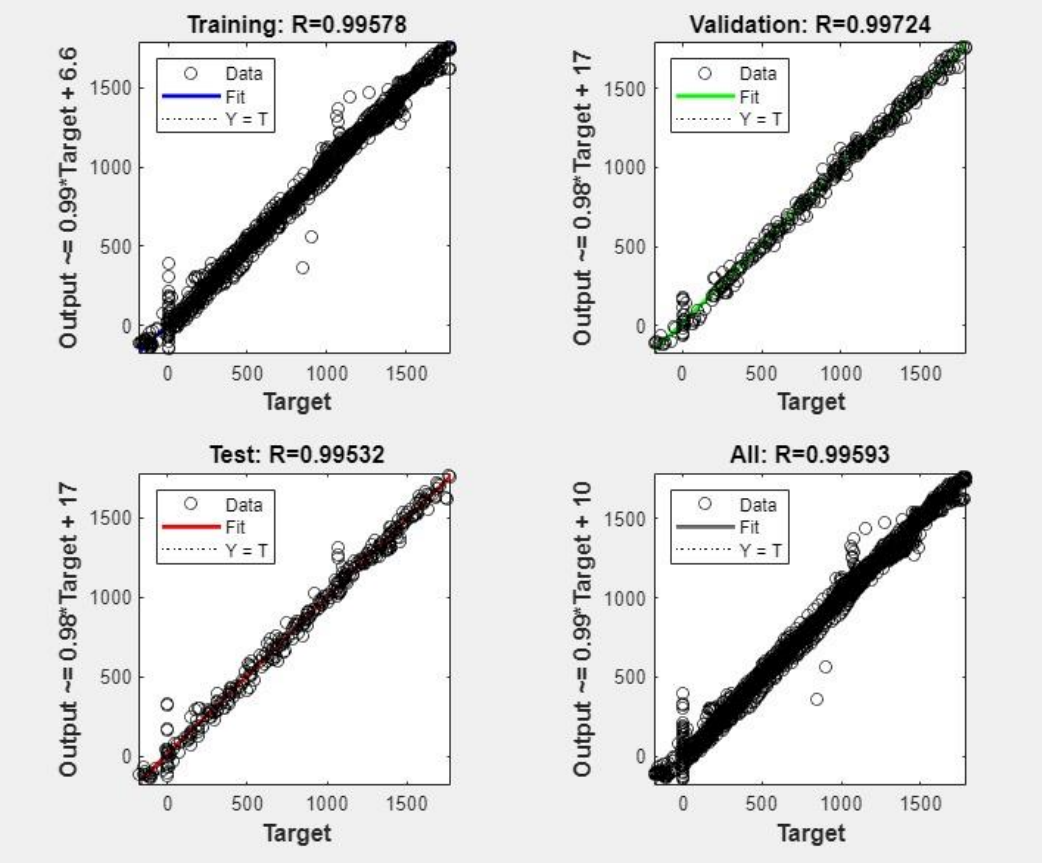

Figure 4. 7 After the fitting operation Regression graph

As seen, after the curve fitting operation, the variables come closer to the slope. This situation made R value closer to one. Another advantage of the fitting at the Synthesis stage, the optimum performance is provided in less epoch. As seen in the Figure 4.12, before the fitting, the best validation performance is occurred at epoch 154.

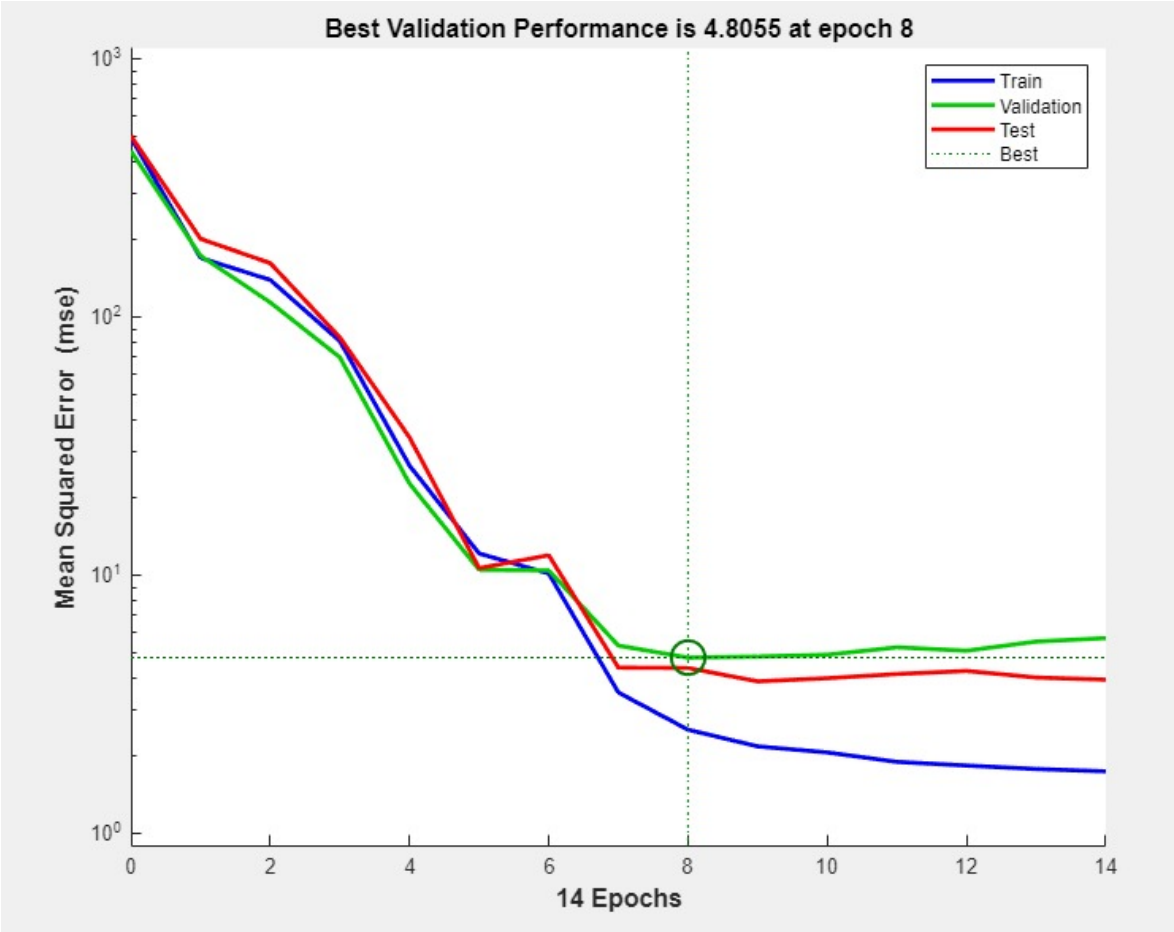

Figure 4. 8 Before the fitting operation Mean Squared Error with respect to epoch

As can be seen in Figure 4.13, the validation performance is occurred epoch fifty with less MSE. So, one can claim that if the system reaches the optimum epoch fast, the MSE decreases.

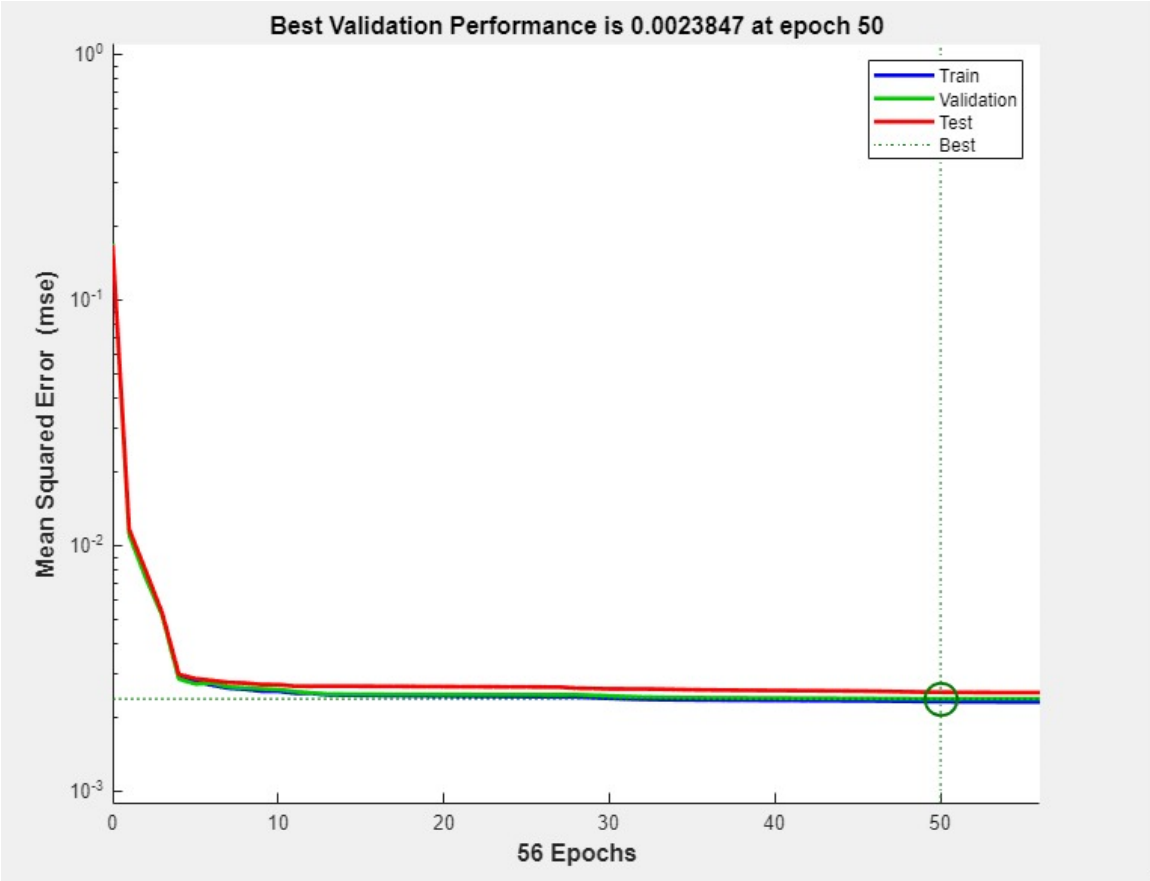

Figure 4. 9 After the fitting operation Mean Squared Error with respect to epoch

One can claim from Figure 4.12 and Figure 4.13, the MSE is decreased when the input variables are fitted with respect to target values. On the other hand, epoch number is increased. This situation is not expected. The expectation is both epoch number and MSE decrease when the input variables are fitted.

Table 8 Comparison of the literature and this work in terms of accuracy

Reference	Training Algorithm	Antenna Type	Accuracy (%)
[13]	LM	Probe Fed Rectangular Patch	96.68
[47]	SCG	Edge Fed Rectangular patch	97.56
[48]	Radial Basis Function Network	Fractal Antenna	98
[49]	LM	Circular Fractal Antenna	98.8
[50]	Back Propagation	Edge Fed Rectangular patch	97.7
[51]	Genetic Algorithm-Coupled ANN	Multi-Slot Hole-Coupled Microstrip Antenna	98.6
[52]	LM	Single-Feed Corner-Truncated Circularly Polarized Microstrip Antenna	98.1
This Work	LM	Notched Square Monopole Antenna	99

As seen at Table 8, proposed ANN algorithm has a better accuracy result with respect to compared studies.

LM, SCG and BR are the MLP neural network training algorithms. This study also required to model the proposed antenna using a non-MLP algorithm. Because of that proposed antenna is also applied to Radial Basis Function Network (RBFN) [48]. To see the difference between MLP and RBFN training algorithm, LM and RBFN are compared. To compare the accuracy of LM and RBFN, the input of the ANN is selected same. For example, the input of the ANN is f_c' and BW' equal to 3.588 and 64.2, respectively. Output of the LM algorithm is L''=22.89, NL''=1.71, NW''= 0.84. When these values are applied to EM simulation, the resulting values equal to 3.549 and 59 for f_c and BW whereas the same input values are applied to RBFN, the output of the RBFN is L''=24.36, NL''=4.66, NW''= 0.46. These values are applied to EM simulations. The output of the EM simulations equal to 3.18 for f_c and 58.4 for BW. For LM, the accuracy of f_c equals to %99.3 and the accuracy of BW equals to %ninety-nine. On the other hand, for RBFN, the accuracy of fc equals to %eighty-nine and the accuracy of BW equals to %90.9. In the Table 9, RBFN The RBFN algorithm has been evaluated with different hidden layers. Hidden layer is denoted as HL.

Table 9 RBFN output of the different hidden layer

HL	L''	NL''	NW''	f_c - EM	BW-EM	Acc.
3	23.12	2.65	0.69	3.505	63	97.6
4	29.12	7.9	0.69	3.095	47.4	86.2
5	27.93	7.95	0.69	2.925	55	81.4
6	28.43	8.86	0.69	2.815	53	78.8
7	28.29	7.55	0.71	2.84	52.8	79.1
8	24.36	4.66	0.46	3.18	58.4	88.6
9	26.32	5.06	0.70	3.15	59	87.7
10	27.17	6.38	0.63	3.04	56.5	84.7

As seen from the Table 9, RBFN which has the eight hidden layer has the most accurate result. LM algorithm is also evaluated with different hidden layer. Table 10 is created to show the output of the LM with different hidden layers.

Table 10 Output of the LM with different hidden layers

HL	L''	NL''	NW''	f_c - EM	BW-EM	Acc.
3	29.54	8.72	0.69	3.449	3.588	97.6
4	23.76	3.42	0.70	3.355	60.5	93.5
5	23.95	3.15	0.67	3.435	62.5	95.7
6	24.45	2.29	0.65	3.32	60.2	92.5
7	25.48	3.69	0.67	3.21	57.9	89.4
8	22.89	1.71	0.84	3.549	64	99.3
9	24.41	1.98	0.64	3.335	59	92.9
10	19.57	6.91	0.82	4.07	55	88.1

As can see from the Table 10, LM which has the eight hidden layer has the most accurate result. Because of that LM which has eight hidden layer and RBFN which has three hidden layers are selected to compare LM and RBFN accuracy performance. At the Table 11 comparison of the LM and RBFN is given.

Table 11 Comparison of the LM and RBFN

Algorithm	L''	NL''	NW''	f_c - EM	f_c'	BW- EM	BW'
LM	22.89	1.71	0.84	3.449	3.588	64	64.2
RBFN	29.54	8.72	0.69	3.449	3.588	64	64.2

As given in Table 8 and Table 9, LM is more accurate when eight hidden layer is used. On the other hand, RBFN is faster than the LM training algorithms. Figure 4.10 shows the EM results of the antennas which are implemented by RBFN and LM.

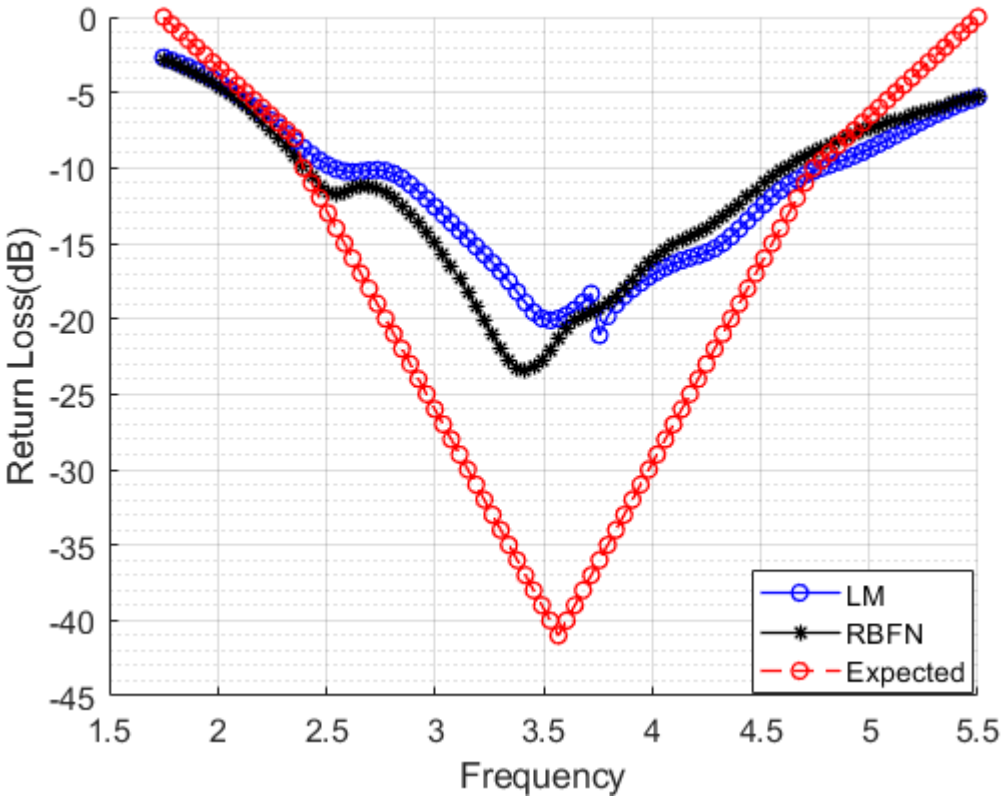

Figure 4. 10 EM results of the antennas which are implemented by RBFN and LM

As seen, the antenna which is produced by LM has the dimensions of L''=22.89, NL''=1.71, NW''= 0.84 showed wider bandwidth performance. Also, these results are closer to desired f_c and BW.

5. Fabrication and Measurement

In order to compare the simulation studies and fabrication results, notched Square Monopole Antenna designed within the scope of this thesis is manufactured. Three notched square monopole antenna is produced. These are UHF band, S band and L band antenna.

5.1. Notched Square Monopole Antenna Fabrication and Measurement

Within the scope of this thesis, antenna production was made in order to compare with simulation studies. The measurements of these antennas were first simulated in HFSS, the measurements obtained from the ANN. Then, the dimensions of the design were sent to the laser cutting manufacturer. The material constituting the antenna is determined as brass. Because brass is the best solder holding material. Figure 5.1 shows the radiating element of the antenna.

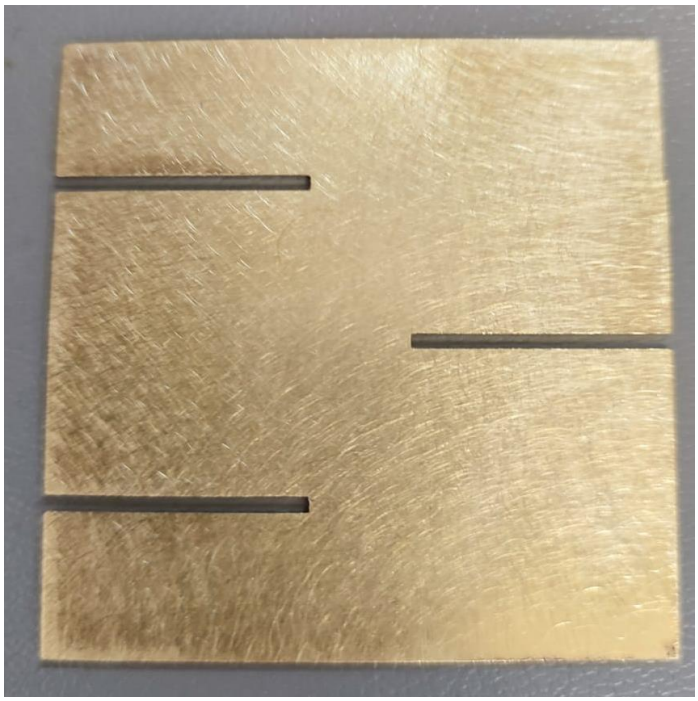

Figure 5. 1 The radiating element of the antenna

Figure 5.2 shows radiating element is connected to SMA connector. At the soldering operation, the brazing machines' temperature should be higher than 450^{o}C, because the brass cools down extremely fast. This situation makes soldering operation hard. Moreover, to have a better soldering performance, the brass is sanded. On the other hand, the SMA connector model can be selected to apply a planar antenna. In this work, panel mount type SMA connector is used.

Figure 5. 2 Radiating element is connected to SMA connector

The antenna is evaluated by network analyzer indoor environment. The network analyzer is calibrated 1 GHz to 4 GHz by 1 MHz steps. The network analyzer is calibrated by matched load, short and open loads. The antenna is measured by low loss coaxial cable which has 0.1dB/m attenuation.

Figure 5.3 shows the antenna is evaluated by network analyzer with ground plane.

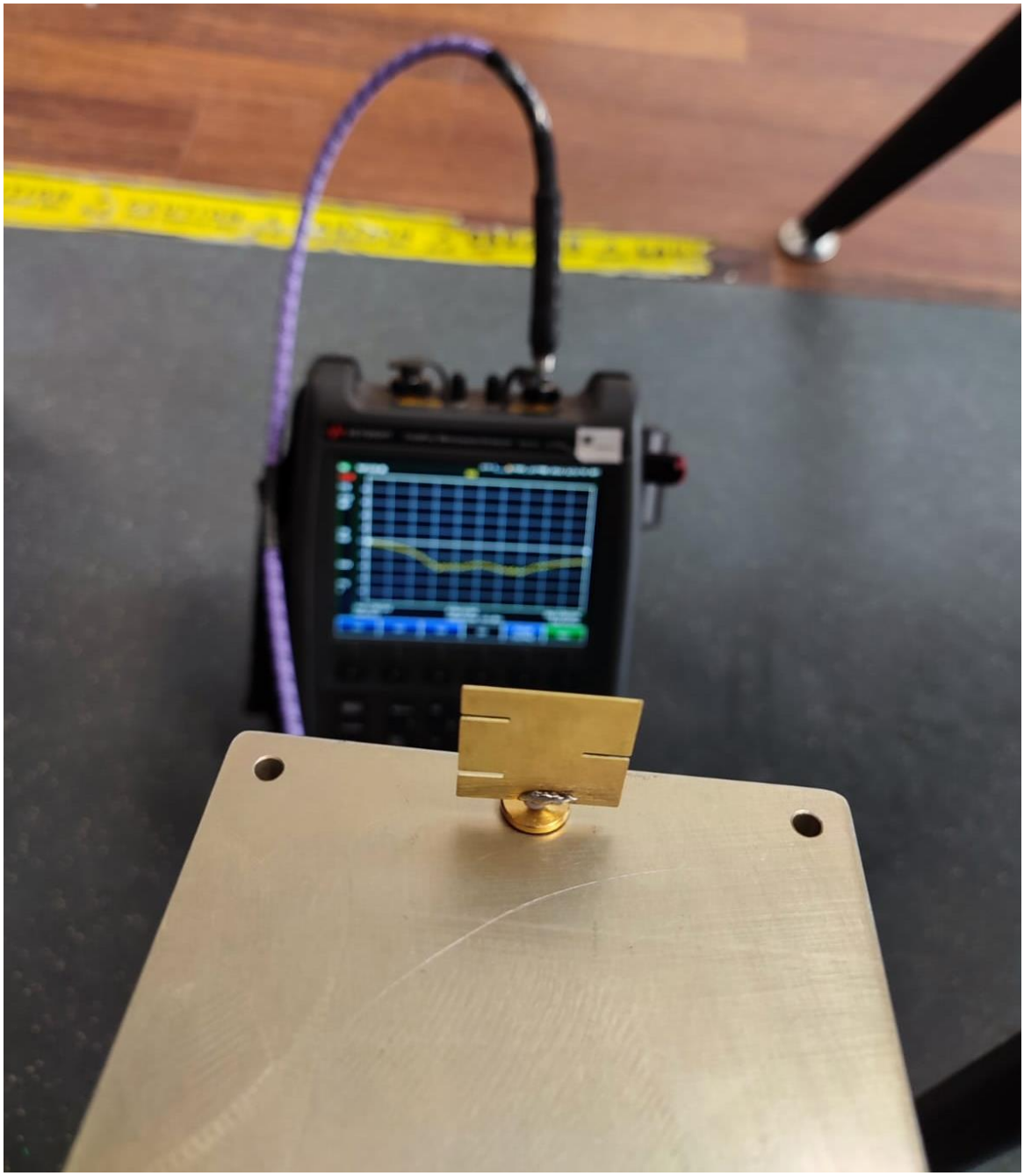

Figure 5. 3 The antenna is evaluated by network analyzer with ground plane

To understand the accuracy of the manufactured antenna and simulated antenna, the S_{11} result is given. S band antenna measurement and simulation result is given below as can be seen from Figure 5.4.

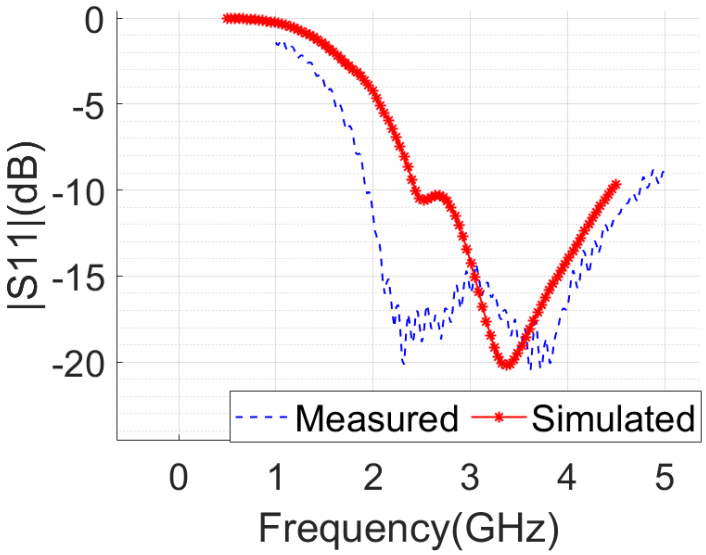

Figure 5. 4 S band antenna measurement and simulation result

As seen, manufactured antenna has wider bandwidth compared to simulated antenna. This is because of sometimes manufacturing techniques make defects. On the other hand, in this production, due to coating of the ground plane boosted antenna's performance. L band antenna measurement and simulation result is given below as can be seen from Figure 5.5.

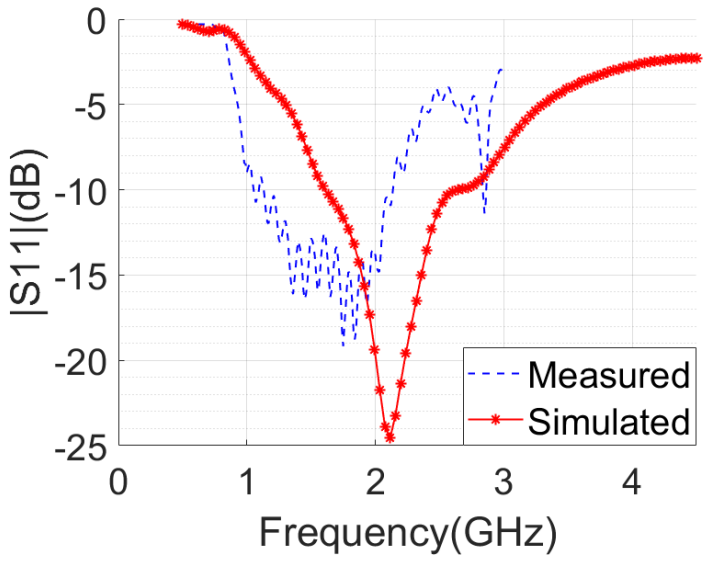

Figure 5. 5 L band antenna measurement and simulation result

As seen, there is a dramatic frequency shift in L band antenna. This situation is happened due to the soldering radiator to SMA connector was not effective. The gap between radiator and ground plane is not equal to designed model.

UHF band antenna is also manufactured. UHF band antenna measurement and simulation result is given below as can be seen from Figure 5.6.

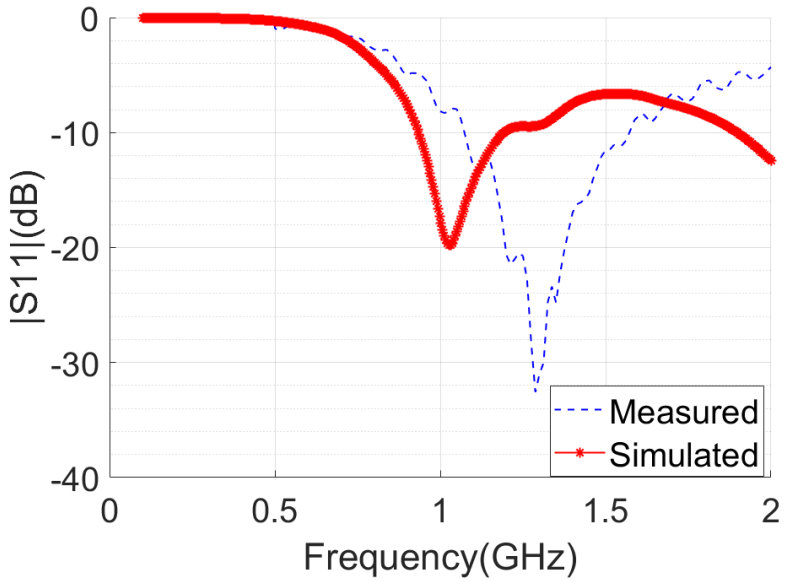

Figure 5. 6 UHF band antenna measurement and simulation result

One can claim that measured and simulated S_{11} values are really close to each other. ANN is manufactured antennas overlaps accurately to their measured and simulated results. There are minimal problems that are can be fixed next manufacturing.

6. CONCLUSION

In this thesis, artificial neural network is proposed for designing notched metal-plate square monopole antenna. S-parameter quantities such as center of frequency and bandwidth are the input values to predict antenna design parameters. In this antenna design produce, notches are used to increase Q value to have a wider bandwidth. ANN system is consisting of the two parts that are synthesis and analysis. The forward side of the ANN process is known as synthesis, while the reverse side is defined as analysis. Because the analysis ANN network is regarded the final stage of the ANN, the data acquired by reversing the input-output data of the synthesis network determines the parameters of the analysis ANN network. As a result, using LM, one may determine the geometric dimensions of the antenna, the length of the notch, and the width of the notch with great precision. The simulation results suggest that the generated ANN models are accurate and dependable, and that they may significantly reduce antenna design process. It is also shown that it can generalize and predict accurate model parameters for data that is not in the training set. Finally, antenna parameters are grouped to make contact between antenna design parameters and S-parameter results. It can be said that while length of the antenna is the most important quantity to tune the antenna frequency spectrum, length of the notch and width of the notch could be used to optimize antenna bandwidth. This study also required to model the proposed antenna using a non-MLP algorithm. Therefore, proposed antenna is also applied to Radial Basis Function Network (RBFN). The hidden layer of the training algorithms is chosen by iterations. The amount of the hidden layer is chosen which has the most accurate EM result.

In future studies, like this antenna, a dual-band notched metal-plate square monopole antenna can be designed using ANN. Also proposed ANN system can be used to tune the antennas' far-field performance.

REFERENCES

[1] H. J. Delgado, "Automated antenna synthesis using neural networks and the finite difference time domain," Ph.D. dissertation, Florida Institute of Technology, Melbourne, FL, May 2003.

[2] R. W. Ziolkowski, N. K. Madsen, and R. C. Carpenter, "Three-dimensional computer modeling of electromagnetic fields: A global lookback lattice truncation scheme," J. Comput. Phys., pp. 360–408, 1983.

[3] M. Salazar-Palma, T. K. Sarkar, L.-E. G. Castillo, T. Roy, and A. Djordjevic´, *Iterative and Self-Adaptive Finite-Elements in Electromagnetic Modeling*. Norwood, MA: Artech House, 1998.

[4] E. Michielssen, J. M. Sajer, and R. Mittra, "Design of multilayered FSS and waveguide filters using genetic algorithms," in *Proc. IEEE Antennas Propagation AP-S Int. Symp.*, vol. 3, Jun. 28–Jul. 2, 1993, pp. 1936–1939.

[5] D. Eclercy, A. Reineix, and B. Jecko, "FDTD genetic algorithm for antenna optimization," *Microwave and Optical Technology Letters*, vol. 16, no. 2, pp. 72–74, Oct. 5, 1997.

[6] S¸. Sagıroglu, K. Guney, "Calculation of resonant frequency for an equilateral triangular microstrip antenna using artificial neural Networks", *Microwave Opt. Technology Lett.*, Vol. 14, pp. 89-93, 1997.

[7] S¸. Sagıroglu, K. Guney, M. Erler, "Resonant frequency calculation for circular microstrip antennas using artificial neural networks", *International Journal of RF and Microwave Computer-Aided Engineering*,Vol. 8, No. 3, pp. 270-277, 1998.

[8] D. Karaboga, K. Guney, S¸. Sagıroglu, M. Erler, "Neural computation of resonant frequency of electrically thin and thick rectangular microstrip antennas", *Microwaves,*

Antennas and Propagation, IEE Proceedings-Vol. 146, No. 2, pp. 155 – 159, April 1999.

[9] K. Guney, S¸. Sagıroglu, M. Erler, "Generalized neural method to determine resonant frequencies of various microstrip antennas", *International Journal of RF and Microwave Computer-Aided Engineering*, Vol. 12, No. 1, pp. 131-139, January 2002.

[10] D. Caratelli, R. Cicchetti, G. Bit-Babik and A. Faraone, "Circuit model and near-field behavior of a novel patch antenna for WLAN applications", *Micowave and Optical Technology Letters*, Vol.49, No.1, Jan. 2007, pp.97-100.

[11] Pandey, Anil. (2019). Design of Compact Dual-Band Planar Antenna for WLAN Systems. *AEU - International Journal of Electronics and Communications*. 13. 516. 10.5281/zenodo.3346704.

[12] Aneesh M., Singh A., Ansari J. A.,Kamakshi, Sayeed SS. Investigations for performance improvement of X-shaped RMSA using artificial neural network by predicting slot size," *Progress in Electromagnetics Research C*., vol. 47, pp. 55-63,2014.

[13] Turker N., Gunes F., Yildirim T., "Artificial neural design of microstrip antennas," *Turk J Elec Eng & Comp Sci*., vol. 14, no. 3, pp. 445-453, 2006.

[14] S. Honda, M. Ito, H. Seki, and Y. Jinbo, "A disc monopole antenna with 1:8 impedance bandwidth and omnidirectional radiation pattern," in *Proc. Int. Symp. Antennas Propag*., Sapporo, Japan, 1999, pp. 1145–1148.

[15] M. Hammoud, P. Poey, and F. Colombel, "Matching the input impedance of a broadband disc monopole," *Electron. Lett*., vol. 29, pp. 406–407, Feb. 1993.

[16] Dubost G and Zisler S. *Antennas a Large Bande*. New York: Masson, 1976.

[17] P.V. Anob, K.P. Ray, and G. Kumar, Wideband orthogonal square monopole antennas with semi-circular base, *IEEE Antennas Propagat Soc Int Symp*, Boston, MA, 2001, pp 294 –297.

[18] M.J. Ammann, Control of the impedance bandwidth of wideband planar monopole antennas using a beveling technique, *Microwave Opt Technol Lett* 30 (2001), 229 – 232.

[19] M.J. Ammann and Z.N. Chen, A wide-band shorted planar monopole with bevel, *IEEE Trans Antennas Propagat* 51 (2003), 901–903

[20] M. Ono and Y. Takeichi, "A one-eighth-wave blade antenna with metal leading edge ," *Antennas and Propagation Society International Symposium*,1974, vol.12, pp.225–228, June 1974

[21] Xiao, S., Wang, B.-Z., Zhong, X. and Wang, G. (2003), Wideband mobile antenna design based on artificial neural network models. *Int J RF and Microwave Comp Aid Eng*, 13: 316-320.

[22] M.J. Ammann, Square planar monopole antenna, *Proc IEE National Conf Antennas Propagat*, UK, 1999, pp 37– 40.

[23] Pandey, Gokarna & Soh, Ping Jack & Mercuri, Marco & Beyer, A. & Vandenbosch, Guy & Schreurs, Dominique. (2013). EM-Based Antenna Optimization for Health Monitoring Radar Sensor.

[24] Mohamed, Abdelhalim & Shafai, Lotfollah. (2011). Performance Study on Modern Ultra Wideband Monopole Antennas. 10.5772/17795.

[25] Seong-Youp Suh, W. L. Stutzman and W. A. Davis, "A new ultrawideband printed monopole antenna: the planar inverted cone antenna (PICA)," in *IEEE Transactions on Antennas and Propagation*, vol. 52, no. 5, pp. 1361-1364, May 2004, doi: 10.1109/TAP.2004.827529.

[26] Cicchetti, Renato, et al. "Wideband and UWB Antennas for Wireless Applications: A Comprehensive Review." *International Journal of Antennas and Propagation*, vol. 2017, annual 2017.

[27] Agrawall, P. A., Kumar, G. and Ray, K., 1998, Wideband planar monopole antennas,- *IEEE Trans*.&- - 46, (2), 294-295.

[28] Rojas, Raul. *Neural Networks: A Systematical Introduction*. Vol. 1. Berlin: Springer, 1996. 1 vols.

[29] Lodge, A.; Xiao-Hua Yu, "Short term wind speed prediction using artificial neural networks," Information Science and Technology (ICIST), 2014 *4th IEEE International Conference* on, vol., no., pp.539,542, 26-28 April 2014

[30] Wang, X.; Sideratos, G.; Hatziargyriou, N.; Tsoukalas, L.H., "Wind speed forecasting for power system operational planning," Probabilistic Methods Applied to Power Systems, *2004 International Conference* on , vol., no., pp.470,474, 16-16 Sept. 2004

[31] Sharma, D.; Tek Tjing Lie, "Wind speed forecasting using hybrid ANN-Kalman Filter techniques," *IPEC, 2012 Conference on Power & Energy* , vol., no., pp.644,648, 12-14 Dec. 2012

[32] Zhao Yue; Zhao Songzheng; Liu Tianshi, "Bayesian regularization BP Neural Network model for predicting oil-gas drilling cost," *Business Management and Electronic Information (BMEI), 2011 International Conference* on , vol.2, no., pp.483,487, 13-15 May 2011

[33] Hagan, M.T., H.B. Demuth, and M.H. Beale, *Neural Network Design*, Boston, MA: PWS Publishing, 1996.

[34] C. A. Balanis, *Antenna Theory: Analysis and Design*. New York: Harper and Row, 1982.

[35] Aneesh, Mohammad & Singh, Ashish & Ansari, Jamshed & Kamakshi, & Sayeed, Saiyed. (2014). Investigations for performance improvement of X-shaped RMSA using artificial neural network by predicting slot size. *Progress In Electromagnetics Research* C. 47. 55-63.

[36] Xinxing Pan, B. Lee and Chunrong Zhang, "A comparison of neural network backpropagation algorithms for electricity load forecasting," *2013 IEEE International Workshop on Inteligent Energy Systems (IWIES)*, 2013, pp. 22-27.

[37] V R. Gross, “Multilayer Perceptrons.” [Online] www.cs.toronto.edu

[38] Kisi, Ozgur & Uncuoğlu, Erdal. (2005). Comparison of three back-propagation training algorithms for two case studies. *Indian Journal of Engineering and Materials Sciences*. 12.

[39] Burden, Frank & Winkler, Dave. (2009). *Bayesian Regularization of Neural Networks. Methods in molecular biology* (Clifton, N.J.). 458. 23-42

[40] D. Marquardt, "An algorithm for least squares estimation of non-linear parameters," *J. Soc. Ind. Appl. Math*., pp. 43141, 1963.

[41] R. Battiti, "First- and second order methods for learning: Between steepest descent and Newton's method," *Neural Computation*, vol. 4, no. 2, pp. 141-166, 1992.

[42] Sun, S., Zhang, G., Shi, J., & Grosse, R. (2019). *Functional variational bayesian neural networks*.

[43] A. K. Kumar, M. Kirti, S. Pani and S. Saxena, "Optimization of Antenna Parameters Using Neural Network Technique for Ku- Band Applications," *2020 7th International Conference on Signal Processing and Integrated Networks (SPIN)*, 2020, pp. 706-709.

[44] M. T. Hagan and M. B. Menhaj, "Training feedforward networks with the Marquardt algorithm," in *IEEE Transactions on Neural Networks*, vol. 5, no. 6, pp. 989-993, Nov. 1994.

[45] Higham, D. J. and N. J. Higham, "*MATLAB guide*," SIAM, Philadelphia, PA, USA, 2005.

[46] Martin Fodslette Møller, "A scaled conjugate gradient algorithm for fast supervised learning, Neural Networks," Volume 6, Issue 4, 1993, Pages 525-533

[47] Malhi, Yuvraj & Gupta, Navneet. (2022). Comparison of Neural Network-Based Soft Computing Techniques for Electromagnetic Modeling of a Microstrip Patch Antenna. 10.1007/978-981-19-0707-4_1.

[48] Kumar, Ashish & Singh, V. (2017). Radial Basis Function Neural Network for estimation of Bandwidth of Antenna. *International Journal of Control Theory and Applications*. 10. 927-932.

[49] Jagtar Singh Sivia, Amar Partap Singh Pharwaha, and Tara Singh Kamal, "Analysis and Design of Circular Fractal Antenna Using Artificial Neural Networks," *Progress In Electromagnetics Research B*, Vol. 56, 251-267, 2013.

[50] Thakare, Vandana & Singhal, P.K.. (2010). Neural network based CAD model for the design of rectangular patch antennas. *Journal of Engineering and Technology Research*. 2. 126-129.

[51] Neog, D. K., Pattnaik, S. S., Panda, D. C., Devi, S., Khuntia, B., & Dutta, M. (2005). Design of a wideband microstrip antenna and the use of artificial neural networks in parameter calculation. *IEEE Antennas and Propagation Magazine*, 47(3), 60–65.

[52] Wang, Zhongbao & Fang, Shaojun. (2014). ANN Synthesis Model of Single-Feed Corner-Truncated Circularly Polarized Microstrip Antenna with an Air Gap for Wideband Applications. *International Journal of Antennas and Propagation*. 2014. 1-7. 10.1155/2014/392843.